AN ABSTRACT OF THE THESIS OF

Bailey F. Keefe for the degree of Master of Science in Microbiology presented on November 15, 2018.

Title: Characterizing *Mycobacterium avium* subspecies *hominissuis* (MAH) Microaggregate Induction of Innate Immunity

Abstract approved:

_____

Luiz E. Bermudez

Bacterial aggregation is a strategy employed by many pathogens to establish infection. *Mycobacterium avium* subsp. *hominissuis* (MAH) undergoes a phenotypic change, microaggregation, when exposed to the respiratory epithelium. This aggregation is an important step in the pathogenesis of the infection, laying the foundation for biofilm formation. We therefore compared how non-aggregated, or planktonic bacteria, and microaggregated MAH can establish lung infections by evaluating mucosal epithelial cell and phagocytic cell responses. Human mucosal lung epithelial cells (BEAS-2B) recognition of MAH mostly occurs through toll-like receptors 1 and 2, which was confirmed through qRT-PCR, reverse-transcriptase PCR, and Western blotting. For both phenotypes, MAP Kinases 1 and 3 are phosphorylated at 30 minutes post infection, and active at the transcriptional level 2 hours post infection. Microaggregate infected BEAS-2B cells up-regulated CCL5, IL-1β, and TNF-α cDNA, while planktonic infected cells only up-regulated IL-1β cDNA at 2 hours post infection. Microaggregates are associated with increased uptake by

macrophages (THP-1 cells) after 1 hour compared to planktonic bacteria (8.83% vs. 5.00%, $P < 0.05$). In addition, the microaggregate phenotype, when internalized by macrophages, had reduced intracellular growth compared to planktonic bacteria. The intracellular replication, however, increased 4-fold as determined at day 6 post infection, when the host cells were treated with microaggregate supernatant, obtained from the incubation of MAH with HEp-2 epithelial cells. Moreover, when microaggregate supernatant was used to form biofilm, planktonic and microaggregated bacteria had higher biofilm mass as compared to wild type MAH in HBSS. Microaggregate supernatant also induces the production of both pro- and anti-inflammatory cytokines, however, MAH infection decreased the level of pro-inflammatory cytokine secretion. The results suggest that epithelial recognition is occurring during MAH infection, and the microaggregate phenotype stimulates an inflammatory response. In addition, the initial bacterial interaction with the mucosal epithelium and development of the microaggregate phenotype has a potential role in pathogenesis, allowing for more robust biofilm formation and establishment of infection.

Characterizing *Mycobacterium avium* subspecies *hominissuis* (MAH) Microaggregate Induction of Innate Immunity

by
Bailey F. Keefe

A THESIS

submitted to

Oregon State University

in partial fulfillment of
the requirements for the
degree of

Master of Science

Presented November 15, 2018
Commencement June 2019

Master of Science thesis of Bailey F. Keefe presented on November 15, 2018

APPROVED:

Major Professor, representing Microbiology

Head of the Department of Microbiology

Dean of the Graduate School

I understand that my thesis will become part of the permanent collection of Oregon State University libraries. My signature below authorizes release of my thesis to any reader upon request.

Bailey F. Keefe, Author

ACKNOWLEDGEMENTS

First, I would like to thank Dr. Luiz Bermudez for the opportunity to pursue a higher level of learning and allowing me to conduct research in his laboratory. I am so grateful for this experience, and his help shaping me into a better scientist. I would also like to thank everyone who has been a part of the Bermudez laboratory for their encouragement, support, and friendship. I would especially like to thank Amy Palmer for her unwavering support, endless guidance, and willingness to always help me. She has pushed me to the finish line. I also want to give Dr. Sasha Rose special thanks for training me, helping me brainstorm, and always answering my plethora of questions.

I want to also thank all of my friends and family for putting up with me and supporting me through this entire process. The constant vent sessions, spontaneous food outings, hiking, adventures, and wine nights are what got me through grad school. I have formed friendships for life, which I will be forever grateful for. Most importantly, thank you mom and dad. You laid the foundation for who I am today, and I am so blessed to have your support and love as parents.

Lastly, I dedicate this work to my Auntie Debbie Franklin and Uncle Greg Wachsler. They were two of my biggest cheerleaders who were taken from this life far too soon. I will always strive to make them proud. May they rest in peace.

CONTRIBUTION OF AUTHORS

Chapter 1: Bailey Keefe wrote the general introduction. Amy Palmer and Luiz Bermudez contributed to the editing process.

Chapter 2: Bailey Keefe helped design the experiments, performed the assays, analyzed the data, and wrote the manuscript. Amy Palmer helped with the editing process, data analysis, and writing the discussion. Luiz Bermudez helped design the experiments, guided the ideas, provided important review of the manuscript, and funded the project.

Chapter 3: Bailey Keefe wrote the discussion and conclusions.

TABLE OF CONTENTS

Page

TABLE OF CONTENTS (continued)

Page

TABLE OF CONTENTS (continued)

Page

LIST OF FIGURES

Chapter 1: Introduction

Mycobacterium avium Complex

Non tuberculous mycobacteria (NTM) refers to mycobacteria that are not a part of the *Mycobacterium tuberculosis* complex or *Mycobacterium leprae* (1). NTMs range from non-pathogenic to opportunistic pathogens, and includes fast and slow growing species that reside in various environmental niches (2). The bacteria have been isolated from numerous water and soil systems with a low pH, low-dissolved oxygen content, and high organic matter content (1). Over 160 species of NTM are linked to causing a form of disease, the majority stemming from pulmonary infections (3). Major pulmonary NTM pathogens consist of *M. kansasii, M. avium, and M. intracellulare* (1). The *Mycobacterium avium* complex (MAC) are the most common species isolated from the respiratory tract and associated with clinical lung infections and disease worldwide (3). MAC species consists of *M. avium* and its subspecies along with *M. intracellulare* (1). *M. avium* is comprised of four subspecies: *M.avium* subsp. *avium*, *M. avium* subsp. *paratuberculosis*, *M. avium* subsp. *hominissuis* (MAH), and *M. avium* subsp. *silvaticum* (4,5). MAC organisms are slow-growing, non-pigmented, acid fast positive, and mildly Gram-positive bacilli that are responsible for chronic localized infections to disseminated disease (1).

Epidemiology

Prevalence of disease caused by NTM varies depending on the geographic region, however, a dramatic increase in prevalence and isolation has been observed in

the United States and Canada within the last 30 years (6). Specifically, in the United States NTM disease is only reportable in 11 states, therefore it is more difficult to assess true disease prevalence. Within the 11 states, reporting for pulmonary NTM is not required. For example, Oregon only requires reporting of non-respiratory disease (7).

Pulmonary NTM disease prevalence and mortality is on the rise in the United States. A population based study conducted in Oregon from 2005-2006 for one or more respiratory isolates found an overall prevalence of 8.6/100,000 persons. This prevalence increased after adjustment for patients aged 50 years or older to 20.4/100,000 persons. This trend holds for more than just the state of Oregon, the highest prevalence is seen in patients over the age of 60. Of the confirmed cases found in the population based study, 87.5% of pulmonary NTM was caused by MAC strains (6,9). Another study conducted in the United States assessed disease mortality from 1999-2010. Over the 11 year period, age-adjusted mortality rates rose for deaths due to NTM from 0.069 to 0.077 per 100,000 person-years. Of the 2990 patients that were deceased during this period, 80.7% were due to pulmonary NTM disease (10). Pulmonary NTM disease is the most prevalent manifestation of NTM infections and the majority of these cases are caused by MAC strains.

Clinical Manifestations and Treatment

MAC strains infect both respiratory and gastrointestinal (GI) mucosa, although the GI route infection is the prevalent form of infection in AIDS patients (11). These infections can cause pulmonary disease, lymphadenitis, disseminated disease, and more uncommonly, skin, soft tissue, and bone disease (12). Infections of

the respiratory tract typically occur in individuals with an underlying lung disease and the pathogenesis is affected by host susceptibility including immune status, genetic background, and presence of localized or generalized lung damage (3,11). Chronic infection of the airways lacking mechanical defenses, such as patients with cystic fibrosis or chronic obstructive pulmonary disorder (COPD), can lead to biofilm formation on the mucosa and destruction of the bronchial architecture (11). Recently, however, there has been a significant increase of respiratory infections caused by MAC strains in patients who are immunocompetent (10). Other symptoms of pulmonary disease caused by MAC strains include chronic or recurring cough, sputum production, fatigue, malaise, dyspnea, fever, hemoptysis, chest pain, and weight loss. The severity of the symptoms also rely heavily on underlying immune status and lung pathology. Comorbidities such as chronic obstructive pulmonary disorder (COPD), bronchiectasis, interstitial lung disease, and HIV are more common in pulmonary MAC infections than in tuberculosis in the United States (10,12). Once biofilm formation has been established in the lungs, infections caused by MAC strains become more difficult to treat.

The treatment of pulmonary disease caused by MAC strains is comparable to tuberculosis treatment regimens in that multiple agents are used over a long period of time. Current guidelines recommend a three-drug macrolide-based therapy. This consists of the macrolide, either clarithromycin or azithromycin, rifamycin (rifampicin or rifabutin), and ethambutol with consideration of streptomycin or amikacin early in the therapy depending on disease severity and stage. Antibiotic therapy should be continued for at least 12 months, and the patient should have a

negative sputum culture before ceasing treatment (3,12). Due to the adverse drug side-effects, patient noncompliance occurs 10-30% of the time. Treatment success rates can be as low as 40% depending on the MAC strain causing lung disease, highlighting the need for safer, more effective treatment regimens (3).

Recently, there has been a change in mycobacterial respiratory therapy from systemic administration to directly targeting the site of infection, such as delivery via inhalation. Aerosolized amikacin in a mouse model for *M. tuberculosis* showed similar efficacy at a lower dose as compared to intra-peritoneal delivery (13). Another new therapy approach is aerosolized liposomes containing amikacin by direct inhalation for treating pulmonary NTM. This directly targets the area of infection and increases intracellular concentrations since macrophages actively phagocytose liposomes. This method of treatment is an alternative that is less toxic and as effective *in vitro* and *in vivo* (14).

MAH Microaggregates

Before biofilm establishment occurs in the lungs, bacteria undergo microaggregation, or a pre-biofilm phenotypic change. Microaggregation is a process where single-cell, or planktonic bacteria come into contact with a mucosal layer and undergo a phenotypic shift to ensure adhesion and invasion of epithelial cells. This is mediated through many bacterial-host receptors and other proteins (15). Specifically, MAH form microaggregates on respiratory epithelial cells after prolonged exposure in clusters of 3-20 bacteria. This phenotype was found to be much more invasive in human respiratory epithelial cells (16). Specific MAH proteins the microaggregates utilize to aid in epithelial adhesion and invasion are microaggregate binding protein

(MBP-1) and microaggregate invasion protein (MIP-1), which modulates the host cytoskeleton (17,18). Many other pathogens also utilize aggregation to aid in pathogenesis. One such pathogen is *Pseudomonas aeruginosa*, which forms multicellular aggregates after interacting with the epithelium. These *P. aeruginosa* aggregates also exhibit hyper invasion after exposure to respiratory epithelial cells (19). MAH microaggregates adhere to the mucosal layer, causing the epithelia to undergo a cytoskeletal rearrangement, and then invade the epithelium in a more efficient manner. After invasion of cells the bacteria will either replicate or escape the epithelial layer, triggering the host innate immune response (11).

Innate Immunity Overview

The respiratory epithelium has numerous defenses against potential inhaled invading pathogens. Airway epithelial cells (AECs) are ciliated which function as the physical removal of foreign particles through constant mechanical movement and coughing (20). Mucus lining the AECs contains numerous antimicrobial agents such as the antimicrobial peptides α- and β-defensins (21). Moreover, the epithelial cells that line the respiratory tract play a key responsive role in innate immune defense against microorganisms by initiating an inflammatory response to recruit phagocytic cells. Many pathogen components act as stimuli to initiate the inflammatory process, such as lipopolysaccharide (LPS), lipopeptides, flagellin, viral or bacterial RNA and DNA (22). Receptors that interact with inflammatory stimuli include CD14, toll-like receptors (TLRs), TNF receptors, and IL-1 receptors. After ligand binding, signal transduction pathways that may be initiated are Mitogen Activated Protein (MAP) Kinase cascades, STAT1, STAT6, and NF-κB (23, 24). These downstream signaling

pathways induce cytokine and chemokine transcription and synthesis. The molecules that may be released from AECs are IL-1, IL-5, IL-6, IL-8, RANTES, GM-CSF, and TGF-β (20).

Toll-like receptor Signaling

AECs contain receptors that respond to specific pathogen-associated molecular patterns (PAMPs) that are present on various bacteria. This discrimination between self and foreign (non-self) partially relies on a highly-conserved family of receptors known as TLRs. TLRs have a conserved Toll/IL-1R (TIR) domain, which consists of about 200 amino acids in their cytoplasmic tails. This domain is crucial for catalyzing signaling cascades within the host cell. The extracellular domain of TLRs is comprised of multiple leucine-rich repeats, which together form a horseshoe shaped structure and play a role in the direct recognition of pathogens. Despite the conservation seen among LRRs, different TLRs can recognize many unique ligands. The subcellular localization of each TLR somewhat correlates to the molecular pattern the TLR will bind. For example, TLR1, TLR2, and TLR4 are located extracellularly on the cell surface within the plasma membrane and will bind foreign antigens before they enter the host cell (22). TLR1 recognizes tri-acylated lipoproteins and TLR2 recognizes di-acylated lipoproteins, therefore both receptors play a role in recognizing mycobacteria, since these are the types of lipoproteins found in the mycobacterial cell wall. Studies have shown that these receptors initiate an immune response in the presence of a 19-kDa native mycobacterial lipoprotein and live *M. avium* as seen through NF-κB activation and the production of TNF-α and IL-6 (25,26). TLR1 and TLR2 form a heterodimer that undergoes a conformational

change after ligand binding that recruits downstream signaling molecules. TLR1/2 utilizes myeloid differentiation primary-response protein 88 (MyD88) and TIRAP that initiate downstream signaling. MyD88 and TIRAP interact with the cytoplasmic TIR domain of the TLRs, and TIRAP is unique to the MyD88 pathway in TLR1/2 signaling. These signaling molecules lead to the activation of MAP Kinase pathways and NF-κB. NF-κB is a transcription factor that, once activated, is released from its inhibitor, and translocates to the nucleus to induce expression of inflammatory cytokines. MAP Kinases ERK1/2, JNK1/2, and p38 may also become active as a result of downstream MyD88 signaling dependent on TLR1/2. These proteins are specific serine/threonine kinases that undergo phosphorylation to become active (22,27). Specifically, ERK1/2 are responsible for cell proliferation and survival, whereas JNK and p38 play a role in induction of apoptosis and cytokine production (28).

Macrophage Interaction

Mononuclear phagocytes, monocytes, macrophages, and mucosal epithelial cells comprise the primary niche of mycobacteria in the airways. Virulent mycobacteria are highly effective at macrophage invasion and survival due to their ability to utilize multiple pathways for uptake and modulate killings mechanisms of the host cell. MAH enters human macrophages *in vitro* through the complement receptor 3 (CR3) on the host cell by direct binding. CR3 is an opsonic protein that binds to mycobacteria, which facilitates this interaction between the bacteria and host phagocytic cell. This invasion pathway allows MAH to avoid certain host defenses such as the production and secretion of reactive oxygen species (ROS) that aid in

intracellular killing. Another mechanism MAH employs is prevention of phagosome maturation and fusion to lysosomes, which prevents the intracellular vacuole from acidifying and killing the bacteria residing there. Intracellular MAH vacuoles remain at a pH of 6.5-6.9, although the bacteria can tolerate a pH of 6.0. Another strategy MAH use in macrophages is the induction of apoptosis, which is triggered by Fas-Fas ligand or TNF-α binding. This mechanism may explain the ability of the bacteria to escape and infect a secondary macrophage. Cytokine and chemokine production by the host macrophage occurs upon MAH infection. Both pro and anti-inflammatory molecules are secreted by macrophages infected with MAH, such as TNF-α, IL-12, RANTES, IL-10, and TGF-β (11,29). RANTES functions as a chemoattractant for circulating macrophages and memory helper T cells (30). TNF-α can lead to triggering apoptosis or further macrophage activation, but IL-10 and TGF-β can interfere with this process. IL-10 also negatively regulates NF-κB activation and inhibits apoptosis, which increases bacterial chances of intracellular survival (29). MAH are effective intracellular pathogens, however, the microaggregate phenotype has not been assessed in the macrophage.

Scope of the master's thesis

The driving question investigated for this master's thesis was why are MAH microaggregates able to establish an infection? Two hypotheses were developed that framed experiments addressing this issue. First, respiratory epithelial innate immune recognition was impaired, which would prevent the chemotactic migration of macrophages. The other possibility is that macrophages would be drawn to the site of infection, but the uptake and removal mechanisms would not be functional. The

following chapter of this thesis aims to answer these questions by targeting intracellular signaling cascade activation in respiratory epithelial cells as well as evaluating macrophage phagocytosis, activation, and intracellular survival.

References

1. Falkinham JO. 1996. Epidemiology of infection by nontuberculous mycobacteria. Clin Microbiol Rev 9:177–215.

2. Tortoli E. 2003. Impact of Genotypic Studies on Mycobacterial Taxonomy: the New Mycobacteria of the 1990s. Clin Microbiol Rev 16:319–354.

3. Stout JE, Koh W-J, Yew WW. 2016. Update on pulmonary disease due to non-tuberculous mycobacteria. Int J Infect Dis 45:123–134.

4. Uchiya K, Takahashi H, Yagi T, Moriyama M, Inagaki T, Ichikawa K, Nakagawa T, Nikai T, Ogawa K. 2013. Comparative Genome Analysis of Mycobacterium avium Revealed Genetic Diversity in Strains that Cause Pulmonary and Disseminated Disease. PLoS ONE 8:e71831.

5. Rossau R, Rigouts L, Mijs W, Portaels F, de Haas P, van Soolingen D, Van der Laan T. 2002. Molecular evidence to support a proposal to reserve the designation Mycobacterium avium subsp. avium for bird-type isolates and "M. avium subsp. hominissuis" for the human/porcine type of M. avium. Int J Syst Evol Microbiol 52:1505–1518.

6. Kendall B, Winthrop K. 2013. Update on the Epidemiology of Pulmonary Nontuberculous Mycobacterial Infections. Semin Respir Crit Care Med 34:087–094.

7. 2016. NTM-TB Insights. Natl Jew Health.

8. Winthrop K. 2011. Pulmonary Disease Associated with Nontuberculous Mycobacteria, Oregon, USA. Emerg Infect Dis 17:1760–1761.

9. Winthrop KL, McNelley E, Kendall B, Marshall-Olson A, Morris C, Cassidy M, Saulson A, Hedberg K. 2010. Pulmonary Nontuberculous Mycobacterial Disease Prevalence and Clinical Features: An Emerging Public Health Disease. Am J Respir Crit Care Med 182:977–982.

10. Mirsaeidi M, Machado RF, Garcia JGN, Schraufnagel DE. 2014. Nontuberculous Mycobacterial Disease Mortality in the United States, 1999–2010: A Population-Based Comparative Study. PLoS ONE 9:e91879.

11. McGarvey J, Bermudez LE. 2002. Pathogenesis of nontuberculous mycobacteria infections. Clin Chest Med 23:569–583.

12. Griffith DE, Aksamit T, Brown-Elliott BA, Catanzaro A, Daley C, Gordin F, Holland SM, Horsburgh R, Huitt G, Iademarco MF, Iseman M, Olivier K, Ruoss S, von Reyn CF, Wallace RJ, Winthrop K. 2007. An Official ATS/IDSA Statement:

Diagnosis, Treatment, and Prevention of Nontuberculous Mycobacterial Diseases. Am J Respir Crit Care Med 175:367–416.

13. Gonzalez-Juarrero M, Woolhiser LK, Brooks E, DeGroote MA, Lenaerts AJ. 2012. Mouse Model for Efficacy Testing of Antituberculosis Agents via Intrapulmonary Delivery. Antimicrob Agents Chemother 56:3957–3959.

14. Rose SJ, Neville ME, Gupta R, Bermudez LE. 2014. Delivery of Aerosolized Liposomal Amikacin as a Novel Approach for the Treatment of Nontuberculous Mycobacteria in an Experimental Model of Pulmonary Infection. PLoS ONE 9:e108703.

15. Beachey EH. 1981. Bacterial Adherence: Adhesin-Receptor Interactions Mediating the Attachment of Bacteria to Mucosal Surfaces. J Infect Dis 143:325–345.

16. Yamazaki Y, Danelishvili L, Wu M, Hidaka E, Katsuyama T, Stang B, Petrofsky M, Bildfell R, Bermudez LE. 2006. The ability to form biofilm influences Mycobacterium avium invasion and translocation of bronchial epithelial cells. Cell Microbiol 8:806–814.

17. Babrak L, Danelishvili L, Rose SJ, Kornberg T, Bermudez LE. 2015. The Environment of "Mycobacterium avium subsp. hominissuis" Microaggregates Induces Synthesis of Small Proteins Associated with Efficient Infection of Respiratory Epithelial Cells. Infect Immun 83:625–636.

18. Babrak L, Danelishvili L, Rose SJ, Bermudez LE. 2015. Microaggregate-associated protein involved in invasion of epithelial cells by *Mycobacterium avium* subsp. *hominissuis*. Virulence 6:694–703.

19. Lepanto P, Bryant DM, Rossello J, Datta A, Mostov KE, Kierbel A. 2011. Pseudomonas aeruginosa interacts with epithelial cells rapidly forming aggregates that are internalized by a Lyn-dependent mechanism: P. aeruginosa aggregation on host cell surface. Cell Microbiol 13:1212–1222.

20. Diamond G, Legarda D, Ryan LK. 2000. The innate immune response of the respiratory epithelium. Immunol Rev 173:27–38.

21. Singh PK, Jia HP, Wiles K, Hesselberth J, Liu L, Conway BA, Greenberg EP, Valore EV, Welsh MJ, Ganz T, Tack BF, McCray PB. 1998. Production of beta-defensins by human airway epithelia. Proc Natl Acad Sci U S A 95:14961–14966.

22. Akira S, Takeda K. 2004. Toll-like receptor signalling. Nat Rev Immunol 4:499–511.

23. Li J-D, Feng W, Gallup M, Kim J-H, Gum J, Kim Y, Basbaum C. 1998. Activation of NF- B via a Src-dependent Ras-MAPK-pp90rsk pathway is required for

Pseudomonas aeruginosa-induced mucin overproduction in epithelial cells. Proc Natl Acad Sci 95:5718–5723.

24. Matsumoto K, Hashimoto S, Gon Y, Nakayama T, Horie T. 1998. Proinflammatory cytokine–induced and chemical mediator–induced IL-8 expression in human bronchial epithelial cells through p38 mitogen-activated protein kinase–dependent pathway. J Allergy Clin Immunol 101:825–831.

25. Takeuchi O, Sato S, Horiuchi T, Hoshino K, Takeda K, Dong Z, Modlin RL, Akira S. 2002. Cutting Edge: Role of Toll-Like Receptor 1 in Mediating Immune Response to Microbial Lipoproteins. J Immunol 169:10–14.

26. Lien E, Sellati TJ, Yoshimura A, Flo TH, Rawadi G, Finberg RW, Carroll JD, Espevik T, Ingalls RR, Radolf JD, Golenbock DT. 1999. Toll-like Receptor 2 Functions as a Pattern Recognition Receptor for Diverse Bacterial Products. J Biol Chem 274:33419–33425.

27. Brown J, Wang H, Hajishengallis GN, Martin M. 2011. TLR-signaling Networks: An Integration of Adaptor Molecules, Kinases, and Cross-talk. J Dent Res 90:417–427.

28. Chang L, Karin M. 2001. Mammalian MAP kinase signalling cascades. Nature 410:37.

29. Rocco JM, Irani VR. 2011. <I>Mycobacterium avium</I> and modulation of the host macrophage immune mechanisms [Review article]. Int J Tuberc Lung Dis 15:447–452.

30. Sangari FJ, Petrofsky M, Bermudez LE. 1999. Mycobacterium avium infection of epithelial cells results in inhibition or delay in the release of interleukin-8 and RANTES. Infect Immun 67:5069–5075.

Chapter 2

Mycobacterium avium subsp. *hominissuis* (MAH) Microaggregate Induction of Innate Immunity is Linked to Biofilm Formation

Bailey F. Keefe[1,2], Amy L. Palmer[1], Luiz E. Bermudez[1,2]

Department of Biomedical Sciences, Carlson College of Veterinary Medicine[1], and Department of Microbiology, College of Science[2], Oregon State University, Corvallis, Oregon.

Manuscript in preparation

Introduction

Infections caused by nontuberculous mycobacterium (NTM) have been globally increasing in the past two to three decades, with infections ranging from chronically localized to potentially fatal disseminated disease. NTM can infect both the respiratory and gastrointestinal tracts, however the route of infection appears to be dependent on both host risk factors and microbial distribution in the environment (1). Organisms of NTM are environmental pathogens that mainly infect immunocompromised hosts, but infection prevalence is increasing, especially in the United States (2). *Mycobacterium avium* subsp. *hominissuis* (MAH) is an opportunistic pathogen found in water systems, such as hospital water tanks and shower head biofilms, and in the soil. Patients with AIDS, cystic fibrosis, and chronic obstructive pulmonary disease (COPD) are at an increased risk for respiratory MAH due to underlying lung pathology (3).

A crucial step of MAH pathogenesis in the lung is the initial adherence and invasion of the respiratory epithelial mucosa. The ability to form biofilm in the lung is a crucial stage of pulmonary disease (3,4). Previous work by Yamazaki et al. showed that *in vitro* exposure of MAH to human bronchial epithelial cells for 24 hours resulted in the formation of microaggregates, consisting of 3 to 20 bacteria clusters, believed to be the initial step to biofilm formation (4). Microaggregates exhibit increased invasion of mucosal epithelial cells and cause lung disease in mice when compared with the single-cell planktonic phenotype (5). Babrak and colleagues used a microarray approach to identify genes that were upregulated when MAH underwent microaggregation formation. Two of the genes investigated encoded

microaggregate binding (MBP-1) and microaggregate invasion (MIP-1) proteins. These were shown to facilitate the initial adherence and invasion to the respiratory epithelium (6). MAH invades mucosal epithelial cells by binding to receptors that trigger a cytoskeletal rearrangement. These bacteria are able to replicate in a vacuole, and ultimately escape the epithelium expressing a virulent phenotype that is highly effective at macrophage infection (3). Since this microaggregate phenotype was discovered, however, the question remains as to how it affects the immune response of the host after initial colonization of the lung.

Toll-like receptors (TLRs) play an integral role in initiating the innate immune response through the recognition of various pathogen-associated molecular patterns (PAMPs). TLRs 1 and 2 recognize lipoproteins located within mycobacterial cell walls (7,8). After ligand binding, TLR2 forms a heterodimer with either TLR1/6 and undergoes a conformational change required for the recruitment of downstream signaling molecules (9). TLR2 uses the TIR-domain containing the adaptor molecule MyD88 (myeloid differentiation primary-response protein 88), which through signaling cascades phosphorylates transcription factor NF-κβ from its inhibitor so that it can translocate to the nucleus and induce expression of inflammatory cytokines such as TNF-α, IL-1β, IL-6, IL-8, and RANTES (9,10). Moreover, the TLR2 pathway stimulates various mitogen-activated protein kinases (MAPK), which induce the transcription of inflammatory molecules leading to the recruitment of phagocytic cells, which are typically macrophages (11).

Mononuclear phagocytes, monocytes and macrophages, are a major niche for mycobacteria survival in their hosts, and are the first cells to migrate to the site of

infection. Virulent mycobacteria are highly efficient at macrophage infection, through the utilization of many pathways, such as complement mediated uptake. After phagocytosis, MAH lives in vacuoles that do not acidify, and do not fuse with lysosomes (3). After escaping the primary macrophage following apoptosis, MAH may infect a secondary macrophage, further spreading the infection (12). Previous work has not investigated the macrophage response to the microaggregate phenotype, or if epithelial immunity initiates signaling to recruit macrophages. In this study the question of how microaggregates are able to establish and evolve into the biofilm phenotype in the airways was addressed.

Materials and Methods

Bacterial strains, growth, and suspensions

Mycobacterium avium subsp. *hominissuis* strain 104 (MAH 104) was originally isolated from the blood of an AIDS patient. Unless otherwise stated, bacteria for experimental procedures were grown and maintained on Middlebrook 7H10 agar supplemented with 10% oleic acid, albumin, dextrose, and catalase (OADC; Hardy diagnostics, Santa Maria, CA) at 37 °C. Single cell bacterial suspensions were generated in PBS + 0.05% tween (PBS-T). Briefly, bacteria grown on Middlebrook 7H10 agar for 5-10 days was re-suspended in PBS-T and then syringe passaged with a 22G, 1.5 inch needle in a 5mL syringe 25 times. The suspension was then observed under the microscope for single bacterial cells and the optical density was measured using a spectrophotometer.

Host cell tissue culture

Human monocyte THP-1 (TIB-202) and Human HEp-2 pharyngeal epithelial cells (CCL-23) were grown in RPMI-1640 media containing 2 mM L-glutamate and 25 mM HEPES (Corning, Manassas, VA) further supplemented with 10 % heat inactivated fetal bovine serum (FBS, Gemini Bio-products, Sacramento, CA). Human BEAS-2B bronchial cells (CRL-9609) were cultured in BEBM media, supplemented with BEGM which contains bovine pituitary extract (BPE), hydrocortisone, human epidermal growth factor (hEGF), epinephrine, transferrin, insulin, retinoic acid, and triiodothyronine (Lonza, Allendale, NJ). All cell types were obtained from the American Type Culture Collection and maintained in 5 % CO_2 and at 37°C for all experiments.

Microaggregate formation of MAH strain 104

Microaggregates were generated as previously described (5,6). Briefly, HEp-2 cells were grown to 80-90% confluency in T75 tissue-culture flasks and pre-treated with 5μg/mL of cytochalasin B (Acros Organics, Thermo Fisher Scientific) for 2 hours. A single cell suspension of MAH 104 was then generated as previously described with an optical density (OD) of 0.300 and used to infect the epithelial monolayer for 24 hours at 37°C and 5% CO_2. As a control, planktonic, or dispersed bacteria, were incubated with cell culture medium in the absence of HEp-2 cells. After 24 hours, the supernatant was poured off, syringe filtered with a 0.22 μm filter and frozen for later use. Next, the remaining monolayer was washed 3 times will ice-cold HBSS to obtain the microaggregated bacteria. This microaggregate suspension was then observed under a microscope for confirmation of the aggregated structures. Differential centrifugation was used to separate out any contaminating HEp-2 cells at 150 x g at 4°C for 5 minutes, and then at 2000 x g at 4°C for 20 minutes. The remaining pellet was re-suspended in 500 μL of PBS-T and then used in subsequent experiments.

Determining the role of toll-like receptor 2 in BEAS-2B cells during bacterial infection

A 48-well plate was seeded at 1 x 10^5 cells per well. Pam3Cys, a synthetic triacylated lipoprotein, was added 24 hours before infection to the appropriate wells as a positive control to ensure TLR2 stimulation (InvivoGen). A neutralizing toll-like receptor 2 (TLR2, InvivoGen) antibody, PAb hTLR2 was added to the appropriate wells per protocol 30 minutes prior to infection. The isotype of the antibody was rat IgG and was diluted 1:40 for a final concentration of 5 μg/mL. Cells were then infected at an

MOI of 10 for 1 and 2 hours with microaggregate or planktonic bacteria. At the indicated time points, supernatant was removed and 400 μL of lysis buffer was added to the wells. The buffer was then serially diluted, and plated for CFU enumeration. For further experiments, PAb hTLR1 (TLR1 neutralizing Ab, rat IgG) was used at the same concentration as PAbhTLR2 to further determine the cellular signaling roles of the TLRs (InvivoGen).

Real time-qPCR of MAP Kinases in epithelial cells and macrophages during MAH 104 microaggregate infection

BEAS-2B cells were seeded at 1 x 10^5 cells/well and 3 x 10^5 cells/well, respectively. Designated wells were pre-treated with PAb hTLR1 and PAb hTLR2 as described in the previous section. BEAS-2B cells were infected with planktonic and microaggregate bacteria and RNA was extracted at 1, 2 and 4 hours post infection using a Qiagen RNeasy kit. RNA was extracted 24 hours post infection from THP-1 cells using the same methods. RNA samples were then DNase (Roche) treated, and cDNA was synthesized using BioRad iScript. All cDNA was made with 100 ng of RNA. cDNA from BEAS-2B cells was then used for real time qPCR employing BioRad SYBR Green, while the THP-1 cell cDNA was used for reverse-transcriptase PCR using AmpliTaq Gold 360 master mix (ThermoFisher). GAPDH was used as the housekeeping gene for both reactions. For RT-qPCR, Cq values were normalized to results from uninfected BEAS-2B cell cDNA and fold-change was calculated to compare gene expression between treatments. RT-PCR products were then resolved on a 1% agarose gel with ethidium bromide and then visualized via a BioDoc-It^2

Imager under UV light. Gels were run at 110 volts for 15 minutes and a 1 kb plus DNA ladder (Invitrogen) was used to determine appropriate band size.

Primers were designed in Primer Blast (NCBI) using the coding sequence (CDS) of the RefSeq mRNA of the designated gene. Gel electrophoresis was employed to test all primers for band intensity and primer dimers. The primers were the following: GAPDH forward, 5'- ATGACATCAAGAAGGTGGTG-3', GAPDH reverse 5'-CATACCAGGAAATGAGCTTG-3' (13); IL-10 forward, 5'-AAGCTGAGAACCAAGACCCAG-3', IL-10 reverse, 5'-GAAGAAATCGATGACAGCGCC-3'; TNFα forward, 5'-CGAGTGACAAGCCTGTAGC-3', TNFα reverse, 5'-GGTGTGGGTGAGGAGCACCT-3' (13); IL-1β forward, 5'-GGAGAATGACCTGAGCACCT-3', IL-1β reverse, 5'-GGAGGTGGAGAGCTTTCAGT-3'; RANTES forward, 5'-TACACCAGTGGCAAGTGCTC-3', RANTES reverse, 5'-GAAGCCTCCCAAGCTAGGAC-3' (14); MAPK3 forward, 5'-CTAAGGAGCGGCTGAAGGAG-3', MAPK3 reverse, 5'-GCCTCAGCAAAGGAGAGAGG-3'; MAPK1 forward, 5'-ATCGCCGAAGCACCATTCAA-3', MAPK1 reverse, 5'-CAGGACCAGGGGTCAAGAAC-3'; MAP2K2 forward, 5'-GAGAGCCTCACAGCATCTCG-3', MAP2K2 reverse, 5'-CACTTCTTCCACCTCGGACC-3'; MAPK8 forward, 5'-CAGGACTGCAGGAACGAGTTT-3', MAPK8 reverse, 5'-CCTGGGAACAAAACACCACCT-3'.

Extraction and enrichment of phosphoproteins from BEAS-2B cells

Confluent monolayers of BEAS-2B cells were infected with both the microaggregate and planktonic phenotypes for 30 minutes. After infection, the monolayers were washed with 50 mM HEPES and then lysed with CHAPS buffer and 1X Halt Phosphatase Inhibitor Cocktail (Thermo Scientific). The lysates were then scraped into a collection tube and placed on ice for 45 minutes. The samples were then centrifuged for 20 minutes at 10,000 x g at 4°C to pellet cell debris. Supernatants were collected and then used in the Pierce Phosophoprotein Enrichment Kit (Thermo Scientific) per the kit protocol to isolate phosphorylated proteins from the samples. Protein concentrations were determined before and after enrichment using a NanoDrop. Phosphorylated proteins were immediately transferred to a low protein binding tube (Eppendorf) and stored in -80°C until use in Western blotting.

Western Blotting for phosphorylated MAP Kinases

Phosphorylated protein concentrations were determined and each target received 7.4 μg of protein. Two times concentrated Laemmli buffer (BioRad) with 5% β-mercaptoethanol was added in a 1:1 ratio to the protein lysates samples and vortexed. Lystaes plus buffer were then boiled for 8 minutes at 96°C to denature the proteins. Mini-PROTEAN TGX protein gels (BioRad) were used and 40 μL of buffer plus protein was added per lane after the cassette was filled with 1X running buffer consisting of trisbase, glycine, SDS, and H_2O. Precision Plus Protein standards ladder (5μL, BioRad) was added for each target tested. The gel was run at 150 volts for 45 minutes and then allowed to equilibrate in Towbin buffer for 20 minutes. Nitrocellulose membranes were cut to fit the gel pieces. Proteins were transferred for

20 minutes at 20 volts semi-dry apparatus. Blocking buffer consisted of 5% nonfat milk in PBS-T and then incubated with membranes for one hour at room temperature on a shaker. After washing 3 times for 10 minutes each in PBS-T, primary antibodies targeting Phospho-p44/42 MAPK (ERK1/2), Phospho-p38 MAPK, and Phospho-SAPK/JNK (Cell Signaling Technology) were added in a 1:1000 dilution to the three membranes. Membranes were incubated in primary antibody overnight and then were washed three times for 10 minutes each with PBS + tween. Secondary antibody 800CW goat anti-rabbit IgG (LI-COR) was added in a 1:10,000 dilution for 1 hour on a shaker. After the wash steps were repeated, the membrane was visualized using a LI-COR imager.

Uptake and survival of MAH 104 microaggregates compared to planktonic bacteria in THP-1 infections

THP-1 cells were counted using a hemocytometer, then seeded at 3 x 10^5 cells/500 µL in a 48 well plate with complete media containing 50 ng/mL phorbol 12-myristate 13-acetate (PMA) and incubated. After 24 hours, media was removed and replaced with fresh complete media and incubated overnight at 37°C. Microaggregates were formed and harvested as previously described then after resuspension in 300-500uL of PBS + 0.05% Tween they were compared to the optical density of a Macfarland standard of 3.0 X 10^8 CFUs/mL. The bacteria were diluted in fresh complete media to achieve an MOI of 10 for 300 µL/well of the tissue culture plate. The infection was then synchronized using centrifugation for 10 minutes at 110 x g, and then placed in the incubator for 1 hr at 37°C. After infection duration completed, media was removed and cells were washed 2x with HBSS. Fresh complete media containing

50ug/mL of amikacin was added for 2 hours at 37°C to remove extracellular bacteria. After antibiotic treatment, cells were washed once more with HBSS and then replenished with fresh complete media. Bacterial uptake by THP-1 cells was determined immediately after antibiotic treatment and wash steps, by adding 400 μL of lysis buffer (0.1% TritonX-100 in H_2O) and considered day 0. Subsequent timepoints were used to determine the survival of MAH 104 at day 2, 4, 6, and 8 if needed with the addition of 400 μL lysis buffer. The cell lysates were serially diluted and plated onto Middlebrook 7H10 agar for CFU determination after 7 days of incubation at 37°C. Complete media was changed at 2, 4, 6, and 8 days.

Biomass of biofilms determined by crystal violet assay

Biofilms were made as previously described with modifications (15). First, microaggregate and planktonic bacteria were made as previously described above. Then biofilms were formed in supernatant, media, and HBSS using solid media grown, microaggregate, and planktonic bacteria. The microaggregate and planktonic phenotypes were centrifuged and re-suspended in the indicated treatments at 3 x 10^8 CFUs/mL. Plate grown bacteria were suspended in media, supernatant, and HBSS at the same concentration. Aliquots of 150 μL were added to the proper number of wells in a 96 well-plate. Biofilms were allowed to form in a dark, 25°C incubator for up to 14 days. Biofilm mass was quantified at day 7 and 14 post formation using the crystal violet assay (16). Absorbance was taken on an Epoch (Biotex) using manufacturer's software for analysis.

Determining cytokine concentrations in microaggregate supernatant and complete media-treated THP-1 cells

A Qiagen Custom Mix-n-Match Multi-Analyte ELISArray Kit was designed and ordered with the following twelve cytokine and chemokine targets: IL-1α, IL-1β, IL-4, IL-6, IL-8, IL-10, IL-12, TNF-α, TGF-β, MIP-1b, IFN-α, and GM-CSF. Each target had 8 wells, allotting for 6 samples and a positive and negative control. The 6 samples consisted of supernatants from planktonic infected, microaggregate infected, and uninfected cells treated with either cell culture media or microaggregate supernatant 24 hours post infection. The ELISA was performed following the kit protocol for cell culture supernatant samples. Twelve standards corresponding with the twelve selected targets were provided for the positive controls. Likewise, twelve detection antibodies were provided in the same manner. Absorbance was taken at 450 nm on an EPOCH (Biotex) using manufacturer's software for analysis. The resulting values were then used to compare absorbance between samples.

Determining cytotoxicity in THP-1 cells upon infection under complete cell culture media and microaggregate supernatant conditions

THP-1 cells were prepared in a tissue culture plate and infected as described in a previous section. Cells were infected using planktonic and microaggregate bacteria under complete cell culture media and microaggregate supernatant conditions. Media (complete media or microaggregate supernatant) was replaced at days 2 and 4 post infection. Supernatants were collected at days 2 and 6 post infection to be used in the Pierce LDH Cytotoxicity Assay Kit (Thermo Scientific) to determine percent cytotoxicity between the different treatments. Appropriate controls were included in

the experimental design. Samples were aliquoted into a 96-well plate and the kit protocol was followed to generate the colorimetric assay. Absorbance was taken at 490 nm and 680 nm on an EPOCH (Biotex) using manufacturer's software for analysis. The 680 nm wavelength was subtracted from 490 nm wavelength in subsequent analysis.

Utilizing the TUNEL assay to determine THP-1 cell apoptosis

The TACS (Trevigen Apoptotic Cell System) *in situ* kit (Trevigen) was used for colorimetric detection of apoptotic DNA fragmentation in macrophage monolayers. THP-1 cells were prepared at 1 x 10^5 cells/well in a 96 well plate in the same manner as described in a previous section. Wells were infected with both phenotypes under complete culture media and microaggregate supernatant. The HT Titer TACS kit was followed per the manufacturer's instructions. The THP-1 cells were prepared and fixed using the monolayer method. A positive control was generated using the TACS-Nuclease and all samples, except the background wells, received the labeling reaction. Reaction kinetics were followed at 630 nm on an EPOCH (Biotex) and once the reaction was stopped using 0.2 N HCl the plate was read at 450 nm using the manufacturer's software for analysis.

Western blotting for Caspase-3

THP-1 cells were seeded and infected as previously described, except at a higher cell/well concentration in a 24-well plate. 6 x 10^5 cells/well were prepared and infected under microaggregate supernatant and complete culture medium conditions. Supernatants and monolayers were spun down and collected at days 0, 2, 4, and 6 post infection for lysis to obtain host cell protein. Cells were re-suspended in 30μL

of 4x Bolt LDS sample buffer (ThermoFisher) containing 10 nM protease inhibitor *N*-ethylmaleimide and Pierce EDTA-free protease inhibitor and boiled for 20 mins at 95^{O}C with periodic vortexing. After complete lysis, 60 μL of water containing 1.0 μM DTT was added to each sample and boiled for an additional 10 minutes. Samples were resolved on 4-12% Bolt Bis-Tris polyacrylamide gels (ThermoFisher) followed by blotting onto nitrocellulose membranes using the iBlot system and reagents according to manufacturer's recommendations. Membranes were blocked for 1 hour with a 5% milk solution in TBS with 0.1% Tween-20 (TBS-T). After blocking, the membranes were incubated with anti-Caspase-3 (D3R6Y) Rabbit mAb (Cell Signaling) and anti-β-Actin (Santa Cruz Biotechnology) primary antibodies at a 1:1000 dilution in 0.5% milk TBS-T solution overnight. Membranes were washed with TBS-T for 10 minutes and incubated with secondary antibodies IRDye 680LT goat anti-mouse and IRDye 800CW goat anti-rabbit (LI-COR Biosciences) at a 1:10000 dilution in 0.5% milk TBS-T for 45 minutes. The membranes were washed twice with TBS-T and then once with water, and analyzed using an Odyssey infrared imager (LI-COR Biosciences) and LI-COR Bioscience Software.

Statistics

Statistical analyses were performed in Microsoft Excel. Data are presented as averages +/- the standard deviation or standard error of the mean. P-values were calculated using a two-sided t test.

Results

Both microaggregate and planktonic phenotypes of MAH stimulate the TLR2 pathway

The microaggregate phenotype of MAH 104 has a higher percent invasion than planktonic bacteria in epithelial cells. Moreover, microaggregates utilize specific proteins MBP-1 and MIP-1 to adhere and invade the respiratory epithelium, however it is unknown if initial adherence results in mucosal immune activation (5,6). To explore if epithelial recognition occurs upon microaggregate infection, a toll-like receptor (TLR) pathway was targeted. Ideally, mycobacteria should be recognized by TLR1 and TLR2 because of the lipoprotein components of their cell walls. Other Gram-positive bacteria, such as *Staphylococcus*, also contain lipoproteins in their outer cell wall and rely on TLR2 for epithelial invasion (17). In these first experiments, TLR2 was either neutralized with an antibody, PAb hTLR2, or stimulated with a lipoprotein agonist (Pam3Cys) in human bronchial epithelial cells (BEAS-2B), in order to determine if this receptor played a role for increased bacterial invasion with microaggregates or planktonic bacteria in the epithelial mucosal cell. Neutralizing or stimulating the TLR2 pathway, however, had no effect on bacterial invasion for either phenotype tested (Figure 1a, b). This result suggests that the invasion pathway of the epithelium is not dependent on the binding of a bacterial component to TLR2. However, this assay does not determine if the intracellular signaling cascade was initiated, which would lead to secretion of chemotactic molecules. Therefore, further investigation of the TLR signaling pathway was needed to determine if the MAH phenotypes inhibit the innate immune signaling.

qPCR of TLR2 signaling pathway genes are activated upon microaggregate infection

Stimulation of the TLR2 pathway initiates many intracellular signaling cascades including NF-κB, MAPK signaling, and apoptosis. After ligand binding, TLR1/2 dimerize and undergo a conformational change to recruit the downstream signaling molecules MyD88 and MyD88-adaptor like (MAL) protein, which activate MAP Kinases (MAPK) and NF-κB. Real-time qPCR was used to determine if there were transcriptional differences between MAPK kinase 2 (M2K2), MAPK ERK1/2 (MAPK1/MAPK3), and JNK1 (MAPK 8) when infected with microaggregates or planktonic bacteria. RNA was extracted from cells with no treatment, TLR1, TLR2, and TLR1/2 blocked by neutralizing antibodies. (Figure 2). Microaggregates increased the transcription of M2K2 more than planktonic bacteria in absence of the blocking antibodies. Neutralization of TLR1, 2, and 1/2 decreased levels of M2K2 gene expression (Figure 2A). Although, neutralization of TLR2 alone in cells infected with planktonic bacteria stimulated similar M2K2 gene expression as cells infected with microaggregate bacteria without neutralization (Figure 2E). This same trend is also seen with MAPK3 (Figure 2G). MAPK8 transcription was elevated with both planktonic and microaggregate infections. Antibody neutralization of the TLR1/2 signaling pathway decreased MAPK3 and MAPK8 gene expression with microaggregate infection (9-fold down to 6-fold), while planktonic infections were not altered by antibody neutralization (Figure 2B, 2D). MAPK3 gene expression was increased during both planktonic and microaggregate infection. As with the other genes tested, use of anti-TLR2 antibody lead to a decreased MAPK3 gene expression during microaggregate infection while no change was seen with planktonic (Figure

2D, 2G). In contrast, MAPK1 gene expression was unaltered by either planktonic or microaggregate infection (Figure 2C, 2F). These data indicate that microaggregate infection stimulates higher gene expression for various MAP Kinase intracellular signaling cascades of the TLR2 pathway. This further supports the hypothesis that microaggregates mainly utilize TLR2 in the initial interaction with the epithelium. Although the intracellular MAPK signaling cascade is transcriptionally active upon MAH infection, this does not provide evidence that the protein has been activated upon infection.

TLR2 signaling pathway is activated in epithelial cells as evidenced by downstream phosphorylation

To assess whether various MAPKs were active at the protein level, phosphorylated proteins were extracted and then enriched from BEAS-2B bronchial cells 30 minutes post infection with either planktonic or microaggregate bacteria. Both MAPK ERK1/2 were phosphorylated (42 and 44 kDa, respectively), and therefore activated after 30 minutes post infection (Figure 3). Although JNK and p38 were also examined, neither protein was phosphorylated and thus not visible after enrichment and subsequent western blot. These observations suggest that both phenotypes of bacterial infection activated TLR2 signaling and specifically induced the downstream MAPK pathway ERK1/2 while other routes of TLR2 signaling were not affected. Epithelial recognition of MAH infection is therefore occurring at both the transcriptional and protein level through TLR2 signaling, although it is still unclear whether downstream chemokine/cytokine secretion and or signaling occurs after the bacterial infection.

Transcription chemokine/cytokine profiles of BEAS-2B epithelial cells during planktonic and microaggregate infection

Reverse-transcriptase (RT) PCR was employed to assess whether chemokine and cytokine transcription occurs in BEAS-2B cells two hours following infection with the different MAH phenotypes. The targets chosen were IL-1β, TNF-α, CCL5, and IL-10. IL-1β and TNF-α are important mediators of the inflammatory response and involved in many cellular activities such as proliferation, differentiation, and apoptosis. CCL5 is a chemokine that is secreted upon microaggregate infection of BEAS-2B cells (18) and is chemotactic towards circulating macrophages. IL-10 has many roles in immunoregulation and suppressing inflammation, such as blocking NF-κβ activity. Of the cytokines tested only IL-1β and TNF-α transcription was apparent during planktonic infection (Figure 4 A-C), while microaggregate infected cells also induced IL-1β, TNF-α, as well as CCL5 (Figure 4D-E). When TLR1 and TLR2 were blocked by specific antibodies, IL-1β, TNF-α, and CCL5 transcription was not observed (Figure 4E). Microaggregated MAH induce CCL5 transcription and secretion, with consequent stimulation of biofilm formation (18). This further supports that upon MAH 104 infection, the epithelial innate immune response is initiated through the induction of the TLR2 and MAPK pathways (Figure 5), allowing for signals to be secreted for recruitment of circulating phagocytes.

Increased invasion of microaggregates in human macrophages compared to planktonic bacterial infection

Once the chemotactic molecules have been secreted, macrophages would migrate to the site of infection to potentially eliminate the bacteria. The phagocytic

cell response had not yet been examined in systems involving the microaggregate phenotype, therefore uptake and survival assays were employed using colony-forming units (CFUs) to determine the percent of invasion and intracellular survival. Microaggregates had statistically significantly higher uptake by THP-1 cells, as compared to planktonic bacteria (Figure 6a). This indicates that bacteria with the microaggregate phenotype are more effective at invading macrophages, however, it is unclear what pathway the bacteria utilize to be internalized by the macrophage, compared to planktonic bacteria. Alternatively, microaggregates may cause the macrophage to become more activated, therefore increasing phagocytosis and further activating intracellular killing mechanisms. Intracellular CFUs for both phenotypes were determined to assess bacterial growth rates within the macrophage up to 8 days post infection (Figure 6b). Planktonic CFUs increased at each day evaluated while microaggregate CFUs did not follow the same replication pattern. Microaggregate CFUs decreased at day 4, suggesting that some intracellular killing did occur, but the bacteria did recover and started to grow at days 6 and 8 post infection. These results show that there is no advantage to the bacteria being in the microaggregate phenotype for surviving within macrophages. Microaggregates, however, have higher percent invasion than planktonic bacteria (Figure 6a). Knowing the microaggregate phenotype exhibits higher epithelial and macrophage invasion, the question was posed as to whether this was due to the initial interaction with epithelial cells *in vitro*. During the microaggregate formation process, single-cell MAH 104 are incubated with HEp-2 epithelial cells for 24 hours. After 24 hours, the microaggregated bacteria will be clumped and loosely bound to the host cells. However, the surrounding

supernatant has not been investigated in further assays for possible influence in the biological interactions. Rather than discarding the supernatant during microaggregate isolation, it was then kept and filter-sterilized to be used in THP-1 uptake and survival assays.

Microaggregate supernatant affects phagocytic survival of MAH infection

Uptake under the microaggregate supernatant conditions held a similar trend as seen in figure 6a, suggesting that the supernatant does not affect uptake, however, there is a possibility that microaggregates enter into the phagocyte in a different mechanism than planktonic bacteria (Figure 7a). In addition, the microaggregate's intracellular growth was much more robust at day 6 post infection increasing up to almost 5 times the CFUs from the initial invading bacteria (figure 7b). This drastic change in intracellular replication implies that the supernatant may modulate either the host or bacterial cells in a way to allow for increased growth. Some hypotheses are the supernatant may induce a more anti-inflammatory response in the macrophages, or induce more cell death allowing for bacteria to escape and infect a secondary macrophage. Taken together, the initial bacterial interaction with the epithelium may play a very important role in the pathogenesis by manipulating the intracellular environment of the macrophage to allow for vigorous growth. Based on the uptake trend and increased survival in THP-1 cells with microaggregate supernatant (Figure 7), uninfected HEp-2 cell supernatant was used as a further control to determine if this response was due to solely the host cell epithelium. The uptake was similar for both phenotypes and the bacteria were unable to thrive intracellularly regardless of phenotype (Figure 8). This further supports the

hypothesis that the initial bacterial-epithelial interaction is key to for establishment of infection. It is not yet known, however, what type of molecule, bacterial or host, that is responsible for this effect.

Biofilm mass increases in the presence of microaggregate supernatant

The next step in the supernatant investigation was to determine how well the bacterial phenotypes formed biofilms in the microaggregate supernatant compared to cell culture media and HBSS. Since an increase in replication was observed in macrophages upon contact with the microaggregate supernatant, it was thought that planktonic and microaggregate bacteria would have a greater biofilm mass in presence of supernatant. This idea fits in the overall hypothesis, in which bacteria coming into contact with the epithelium, then releasing chemotactic signals to recruit macrophages, causing about 10% of the bacteria to be ingested. The bacteria that are intracellular are then able to thrive intracellularly, whereas the bacteria that aren't ingested begin biofilm formation in the lung airway. After normalization, the biofilms formed in the supernatant have statistically significantly higher absorbance, i.e. mass, than the plate grown wild-type bacteria left to for biofilm in HBSS (Figure 9). These data indicate that the model used is associated with increase formation of robust biofilm for both planktonic and microaggregate bacteria when left in the microaggregate supernatant compared to HBSS. The plate-grown bacteria did not exhibit more robust formation when in the supernatant, suggesting that the initial incubation with host cells is probably key in the supernatant response.

Microaggregate supernatant causes altered cytokine secretion profiles compared to complete media during MAH infection

Since robust intracellular growth was seen under supernatant conditions versus complete media, a custom ELISA kit was designed with 12 targets to investigate cytokine levels. The 12 targets chosen were: IL-1α, IL-1β, IL-4, IL-6, IL-8, IL-10, IL-12, TNF-α, TGF-β, MIP-1β, IFN-α, and GM-CSF. These cytokines were picked because of their diversity of their involvement in many inflammation processes, being both pro- and anti-inflammatory. THP-1 cells were infected with either microaggregate or planktonic bacteria under supernatant or cell media conditions. Uninfected cells treated with complete media and supernatant were included as controls to determine if the supernatant alone caused a cytokine response. Eight of the targets stimulated cytokine production, which were IL-1β, IL-6, IL-8, IL-10, TNF-α, TGF-β, MIP-1β, and GM-CSF (Figure 10). IL-1α, IL-4, IL-12, and IFN-α cytokines were not stimulated under the experimental conditions tested (not shown). Absorbance was compared to that of uninfected cells incubated with complete culture media. Supernatant alone induced the highest production of IL-6, TNF-α, and GM-CSF. Higher fold-change was observed for infected supernatant treated cells in IL-1β, TGF-β, and MIP-1β production. IL-8 production was similar across all treatments. Taken together, these results show that the cellular response to supernatant is complex, showing evidence for both inflammatory and anti-inflammatory pathways through IL-10 and TGF-β production, which may block or inhibit some pro-inflammatory processes.

Microaggregate supernatant increases macrophage cytotoxicity over time

Since microaggregate supernatant treated THP-1 cells show an increase in bacterial intracellular replication, cellular cytotoxicity was assessed under these same conditions using the lactate dehydrogenase (LDH) assay. At day 2 post infection, complete media treated cells induced more cytotoxicity than microaggregate supernatant treated cells. Planktonic infected cells under complete media conditions at day 2 also had higher LDH release, at about 27 percent cytotoxicity. At day 6 post infection, however, microaggregate supernatant treated cells were more cytotoxic regardless of the bacterial phenotype they're infected with, showing about 20 percent cytotoxicity. This result suggests that microaggregate supernatant delays cellular cytotoxicity, allowing for the bacteria to hide and replicate intracellularly, although it is not known how the host cell killing mechanisms are modulated under this treatment.

Microaggregate supernatant induces late-stage apoptosis in phagocytic cells

To determine if microaggregates or microaggregate supernatant induce macrophage apoptosis, DNA fragmentation and caspase-3 activation were targeted. The Trevigen Apoptotic Cell System (TACS) *in situ* kit was used for colorimetric detection of DNA fragmentation in cells infected with planktonic and microaggregates under microaggregate supernatant or complete media treatments. Staining for DNA fragmentation was performed at days 2 and 6 post infection. Overall, there were minimal differences between apoptosis levels in the cells infected with either planktonic or microaggregated MAH. Complete culture media alone does not induce apoptosis, since infected cells under these conditions at day 2 mirrored

background levels, showing just under 20% fragmentation-positive. However, supernatant treated cells that were infected induced similar percentages of DNA fragmentation, around 40%, at days 2 and 6 post infection (Figure 12). Interestingly, microaggregate supernatant incubated with cells induces apoptosis at day 6 that parallels the level of infected cells, suggesting that there is a component present in this microaggregate supernatant that turns on cellular apoptosis signals. DNA fragmentation indicates late stage apoptosis, therefore early stage apoptosis was also assessed to determine when apoptosis is initiated. This was done by assessing if there is a decrease in the protein expression of pro-caspase-3, a pre-cursor to the intracellular signaling cascade. Band expression ratios (Caspase-3/Actin) indicated that overall, microaggregates have a higher expression of the pro-protein, except after initial infection under supernatant conditions (Figure 13). Supernatant treated cells seemed to have slightly lower Caspase-3 expression than those treated with media. Caspase-3 is an initial indicator that apoptosis is occurring, an early onset decrease of the protein expression would make sense since DNA fragmentation was also seen at day 2 when cells were infected under supernatant conditions.

Discussion

With the prevalence of *Mycobacterium avium* subsp. *hominissuis* (MAH) respiratory infections increasing among people with underlying lung conditions as well as immunocompetent individuals, it is important to develop a better understanding of how MAH interacts with both epithelial and phagocytic cells in the lung environment. Microaggregation of pathogenic mycobacteria is a potential precursor to biofilm formation and are associated with clinical cases of lung infections (1,3,19). This ability to form microaggregates may explain why infections are established and contribute to pathogenesis. Previous work from the laboratory (5,6) have shown MAH microaggregates invasion of naïve BEAS-2B bronchial epithelial depends on the interactions of MBP-1 and MIP-1, and with host cell protein filamin A. These initial interactors do not describe how the host cell reacts to contact and invasion of these bacteria nor how phagocytic cells interact with microaggregates.

To understand how host cells respond to the microaggregate phenotype we investigated the TLR2 pathway for mycobacterial pathogen associated molecular patterns (PAMP) recognition and innate immunity activation in mucosal lung epithelial cells (7,8). MAH invasion was not dependent on the TLR2 receptor being neutralized or hyper-activated with either planktonic or microaggregate bacteria, unlike other pathogens such as *Staphylococcus aureus* (17). As we have observed before MAH microaggregates use MBP-1 for initial binding to host cells, and blocking this protein prevents effective invasion (5,6). Although, it does not exclude the importance of the TLR2 pathway for microaggregate recognition. Gene

expression analysis of TLR2 cascade pathways shows that microaggregates stimulate transcription of MAPK kinase 2, MAPK1/MAPK3, and MAPK8 compared to planktonic bacteria. Using phosphorylated protein capture we tested for activation of MAPK Kinase 2, MAPK 1/MAPK3, and MAPK8. Both planktonic and microaggregate phenotypes stimulated the MAPK 1/MAPK3 pathway but not MAPK8. Phosphorylation of TLR2 cascade pathway proteins show activation, not only gene transcription, at the protein level. Since the same pathway was stimulated by both planktonic and microaggregate phenotypes we determined if different cytokines/chemokines are being secreted by epithelial cells. CCL5, TNF-α, and IL-1β were chosen because of the chemotactic and macrophage activation potential. IL-1β was induced in both planktonic and microaggregates. Microaggregates also stimulated CCL5, suggesting chemotaxis is occurring. This macrophage chemotactic molecule has been shown to be important for MAH to progress into biofilm formation, by stimulating microaggregate formation (18). TNF-α was also induced by microaggregates raising the possibility of its participation in the induction of apoptosis through caspase-8/3 or NF-κB activation. Epithelial recognition is not impaired, and microaggregates depend on the TLR pathway to initiate an innate immune response. Overall, microaggregates induce more inflammatory effects on epithelial cells than planktonic bacteria meaning the phenotype of grouping bacteria causes more cellular responses for attracting macrophages.

MAH microaggregates were shown to initiate epithelial innate immunity, releasing signal to recruit macrophages to the site of infection. This action is important for MAH disease progression allowing the bacteria to hide in the

macrophage and become mobile, spreading to surrounding tissues. We examined the uptake of microaggregates and overall survival of the pathogen in macrophages. While microaggregate invasion was shown to be greater than planktonic bacteria as seen in epithelial cells, microaggregates were unable to thrive intracellularly. We were only able to observe growth of microaggregates when the original supernatant that was generated in the formation of microaggregates on the epithelial mucosal cells was applied to these infections leading us to conclude that the initial interaction of bacteria to epithelial cells has generated some important modulator that promotes improved microaggregate survival in macrophages. This modulation by the microaggregate formation supernatant may be associated with the inability of macrophages not properly removing the bacteria from the infection site.

MAH have the ability to form biofilms which can impair the efficacy of treatment and bacterial clearance by the host. Microaggregation is potentially a precursor step to the formation of these biofilms. Here we observed that supernatant collected from the initial formation of microaggregates on epithelial cells caused increased biofilm mass over 14 days. In addition, microaggregate derived biofilm is increased by its formation supernatant, however plate grown bacterial biofilms were not affected by the microaggregate supernatant. The finding that microaggregate survival inside macrophages is improved with the presence of supernatant, and raises a possibility that a component of the supernatant released from the interaction of MAH and epithelial cells plays a major role in microaggregate virulence. Epithelial cells can be exporting signaling molecules that are interacting with the macrophages, or alternatively, signaling molecules from bacteria are altering the behavior of either

bacteria or macrophages. Future investigations must be carried out with microaggregates supernatant to determine how MAH infections are affected.

To help elucidate the effects of microaggregate supernatant on macrophages infected with planktonic and microaggregated MAH, a cytokine profile was examined. The cytokines investigated are known to be involved with both inflammatory and anti-inflammatory pathways. Macrophages treated with supernatant induced more cytokines than those treated with complete culture media, regardless if the cells were infected or not, suggesting supernatant alone stimulates an immune response. We observed that during infection with either bacteria phenotype pro-inflammatory cytokines such as TNF-α, IL-6, and GM-CSF were reduced compared to just supernatant alone. This pattern of cytokine levels demonstrated direct bacterial interference with normal macrophage cell signaling pathways. MAH is actively reducing pro-inflammatory signals to prevent typical intracellular killing mechanisms, thus allowing MAH to remain resilient to phagocytosis mediated killing and to hide intracellularly. Anti-inflammatory cytokines are also induced during supernatant stimulation and are slightly reduced with MAH infection such as IL-10 and TGFβ. IL-10 and TGFβ can interfere with the macrophage response to TNF-α allowing for bacterial survival. IL-10 also negatively regulates NF-κB activation preventing transcription of cytokines/chemokines (12). Moreover, macrophages that were isolated from patients infected with MAH showed an increase in IL-10 production as compared with healthy controls, and this immunosuppressant advanced the infection (20). We have demonstrated that MAH microaggregates with microaggregate supernatant actively affect cytokine profiles of macrophages

potentially preventing apoptosis and other cellular processes. This cytokine response is early, within 24 hours post infection but the timing of inflammation/anti-inflammation is unknown. These fluctuations of cytokines could help explain how microaggregates are able to survive in macrophages and lead to MAH ultimately infecting immunocompetent individuals and those with underlying conditions.

Another important mechanism for mycobacterial pathogenesis is the ability to control macrophage death pathways. It is thought generally that apoptotic cell death can be bactericidal, while necrosis may facilitate bacterial dissemination, although MAH and *M. tuberculosis* have been shown to survive apoptosis of macrophages, allowing the bacteria to escape the dying cells and infect neighboring naïve macrophages (21,22). The capability to control and manipulate the timing and mechanism of death in infected host cells plays an important role for many microbial infections, such as *M. tuberculosis* and *Legionella pneumophila* (23,24). Here we demonstrate the ability of MAH to modulate necrosis and apoptosis on presence of microaggregate supernatant. During early MAH infection, cytotoxicity of macrophages culture media exposed bacteria was increased compared to microaggregate supernatant. It is only after late stage infection of macrophages do we see an increase in cytotoxicity. This demonstrates that the supernatant is delaying the effects of necrosis in these macrophages upon infection potentially allowing for the bacteria to replicate and survive in the cells. We then investigated if MAH microaggregates modulate apoptosis through DNA fragmentation and Caspase-3 activation. DNA fragmentation represents late apoptosis and Caspase-3 is a precursor to the intracellular cascade leading to apoptosis. In early stages of infection,

regardless of phenotype, microaggregate supernatant caused an increase in apoptosis while culture media treated macrophages had low levels that mirrored the background in apoptosis. During late stage of infection, MAH incubated with culture media have similar apoptosis levels as all supernatant treated macrophages including uninfected cells. Interestingly, cells treated with supernatant had high levels of apoptosis that matched infected cells at day 6. As seen from the cytokine profiling data, supernatant alone induces more production of TNF-α, which can initiate apoptosis (25). *M. avium* induced apoptosis is partially dependent on TNF-α since other work has demonstrated in the presence of an anti-TNF-α antibody, apoptosis was reduced 17% (26). Perhaps the apoptosis levels seen during the late stage is from cells aging and become more susceptible to cellular death. Our own data shows that uninfected macrophages treated with culture media over the entirety of the experiment do not spontaneously undergo apoptosis and in fact remain similar to background levels. We also wanted to determine Caspase-3 activation during microaggregate and supernatant infection. Generally, supernatant treated cells had slightly lower expression of the pro-protein. Interestingly, microaggregate infected cells plus supernatant had less expression after initial infection, indicating that some caspase-3 activation occurs early in the infection time course. Other work has shown that an *M. avium* protein causes early caspase-3 activation in macrophages (27). Supernatant treated cells had less pro-caspase-3 expression, more apoptotic DNA fragmentation, and delayed cytotoxicity suggesting that there may be a component in the supernatant that triggers cell death pathways.

MAH microaggregates were studied to determine the effect of the microaggregate phenotype on epithelial cell and macrophage infection. These cell types match the sequence of disease progression in the host. Taken together, our data convincingly demonstrates that MAH microaggregates uniquely alter cellular responses such as improved intracellular growth, enhanced biofilm formation, and increased secretion of pro- and anti-inflammatory cytokine secretion when compared to planktonic MAH in presence of their formation supernatant. We hypothesize that the component responsible for this altered host response is secreted during microaggregate formation, either by epithelial cells or the bacteria themselves. This unknown component deserves further investigation to elucidate its source, identity, and function.

Chapter 3: Discussion and Conclusions

Overview

MAC strains are opportunistic pathogens that reside primarily in environmental sources. These bacteria are mostly responsible for lung infections which can lead to various types of pulmonary disease. Mycobacteria are able to undergo biofilm formation in the lung airways, which are then much more resistant to treatment. One strain of MAC, *M. avium* subsp. *hominissuis* (MAH), has been extensively studied and shown to undergo a pre-biofilm forming phenotype called microaggregation that is hyper virulent both *in vitro* and *in vivo*. There is a gap in knowledge as to how the immune systems responds to these aggregates and as a whole how biofilms are able to be established. The question was posed as to how MAH microaggregates interact and modulate the host immune system to provide a clearer picture behind the mechanism for pathogenesis.

Optimizing protocols

Generation and isolation of MAH microaggregates has been previously established by a former laboratory member, Dr. Lmar Babrak. I adapted a few small modifications to this protocol, the first being not re-suspending the bacterial pellet after centrifugation until the bacteria were ready to be used in an assay. This prevented losing any turbidity, since the amount of microaggregates isolated was usually very low and I did not have enough to perform an optical density reading, which requires 0.5-1.0 mLs. To prevent bacterial loss to plastic tubing, I also utilized PBS + 0.05% tween 20 for bacterial suspensions and dilutions in later experiments. Generating planktonic and microaggregated bacteria required extra planning when

performing assays, since the process requires a confluent epithelial monolayer and 24 hours of incubation.

Before beginning the experiments of my project, I first had to become comfortable with the microaggregate formation process and tissue culture. I needed to get accustomed to the MAH growth cycle, generating a single-celled suspension, and acid fast staining. Moreover, this was my first experience with cell tissue culture and I needed to have a strong sense of different cell type growth patterns as well as seeding plates, flasks, and passaging the cells while keeping a sterile technique. I had to work with both suspended and monolayer forming cells, although the techniques only varied slightly between cell lines. When performing the macrophage uptake and survival assays, I had to learn how to generate consistent multiplicities of infection (MOIs) and prevent the bacteria from clumping in the inoculums to get accurate CFU readouts. Another skill that required trial and error runs was designing primers for real-time qPCR. This was key for accurate qPCR experiments, so that only one band was amplified and consistent Cq values were generated between biological replicates. Overall, I learned many techniques and how to tailor them to my project.

Experimental Process

Why do MAH undergo microaggregation, or in other words, why does the host allow the bacteria to undergo aggregation in the lung airways before clearance via immune mechanisms? This question drove the subsequent investigation of my project. Some potential hypotheses were that macrophages were not being drawn to the site of infection, meaning there was no signal from the mucosal epithelial cells because MAH microaggregates may interfere with epithelial recognition. Another

possibility is that macrophage uptake and removal mechanisms are not properly functioning, potentially due to something the bacteria are secreting. Pathogens are typically highly adapted at modulating the host immune response, therefore I investigated the *in vitro* mechanism of how MAH microaggregates establish an infection.

The first step in my research was to determine if the TLR1/TLR2 heterodimer play a role in microaggregate invasion and recognition in the respiratory epithelium. In order to test this, I decided to use neutralizing antibodies to block receptor activation, however, I needed to determine what a good downstream read out for TLR activation would be. TLR2 utilizes the MyD88 intracellular signaling cascade, so I first tried to target MyD88 and TIRAP activation via PCR on cDNA from human respiratory epithelial cells. Unfortunately, after troubleshooting many different primer sets, I was unable to get any amplification for these two genes. Therefore I moved onto the downstream MAP Kinases and after finding successful primer sets, I was able to run real-time qPCR to determine changes in gene expression. After seeing transcriptional activity of the various MAP Kinase's, I wanted to discern if any of these proteins were becoming activated via phosphorylation. This process happens very quickly intracellularly, so protein was extracted and enriched at 30 minutes post infection. As a final readout to confirm that epithelial recognition did in fact occur, conventional PCR was used to see if cytokine and chemokine transcription was induced upon MAH infection. I was able to show that MAH microaggregates induce epithelial recognition, and even in a more inflammatory manner.

While assessing the epithelial immune response, I simultaneously was establishing a baseline for macrophage uptake and survival. The first round of uptake and survival assays looked at percent invasion after a one hour infection and then survival after 2 and 4 days. Initially after performing these experiments roughly 6 times, intracellular growth after 4 days was not observed with media changes every 2 days and observing the monolayer for significant cell loss. Some possible explanations for why this occurred were that microaggregates may be overly activating the macrophages due to the pre-incubation with cell culture media, the bacteria may need longer than 4 days to thrive intracellularly, and does the supernatant that the microaggregates were formed in play a role in their infectivity. I extended the survival assay up to 8 days post infection and found that the planktonic phenotype was able to grow inside the host cells after 6 days. Then I utilized the microaggregate supernatant in place of complete culture media to treat the macrophages and found that microaggregates were able to thrive intracellularly. This finding led me to investigate other aspects of microaggregate infectivity such as biofilm formation, cytokine profiling, and cell death pathways under this microaggregregate supernatant. I employed the crystal violet assay to stain for biofilm mass of the bacteria under different media conditions, and this experiment was able to determine biomass levels since crystal violet is able to stain extracellular matrix as well as bacteria. To determine the cytokine profile under microaggregate supernatant, I designed a custom ELISArray kit with 12 targets, which provided an in depth picture of the cytokine response. However, determining cellular cytotoxicity and death pathways proved to be a challenge. I used the colorimetric lactate

dehydrogenase (LDH) assay for cytotoxicity, and it took a couple runs to get the controls in the correct range to produce a viable result. Targeting apoptosis, on the other hand, was more difficult. I tried using flow cytometry and florescence microscopy to stain for Annexin V and propidium iodide. The issue with antibody staining on the flow cytometer was that the cells had to be fixed beforehand, which actually interfered, or washed the staining away. The kit I was attempting to use was also not designed for cells in a monolayer, therefore this may be why I was unable to detect any positive staining under the florescent microscope. To determine if apoptosis was occurring during microaggregate infection with their supernatant, I utilized a colorimetric assay for TUNEL positive cells as well as western blotting for Caspase-3 protein expression.

Overall, I established an *in vitro* model for the initial stages of microaggregate infectivity that include epithelial recognition, the macrophage response, and biofilm formation. The initial interaction with the respiratory epithelium during the microaggregate formation process seems to be key in their pathogenesis by modulating the macrophage to allow for more robust intracellular growth, inducing anti-inflammatory cytokines that could potentially interfere with inflammatory processes, and generating more biofilm formation. Taken together, there is a benefit for this organism to form these microaggregates to increase infectivity and ultimately progression of disease. Our increased understanding of how MAH interacts and infects epithelial cells and also eventually macrophages allows for potential pathway targets for therapeutic agents to disrupt MAH virulence.

Figures

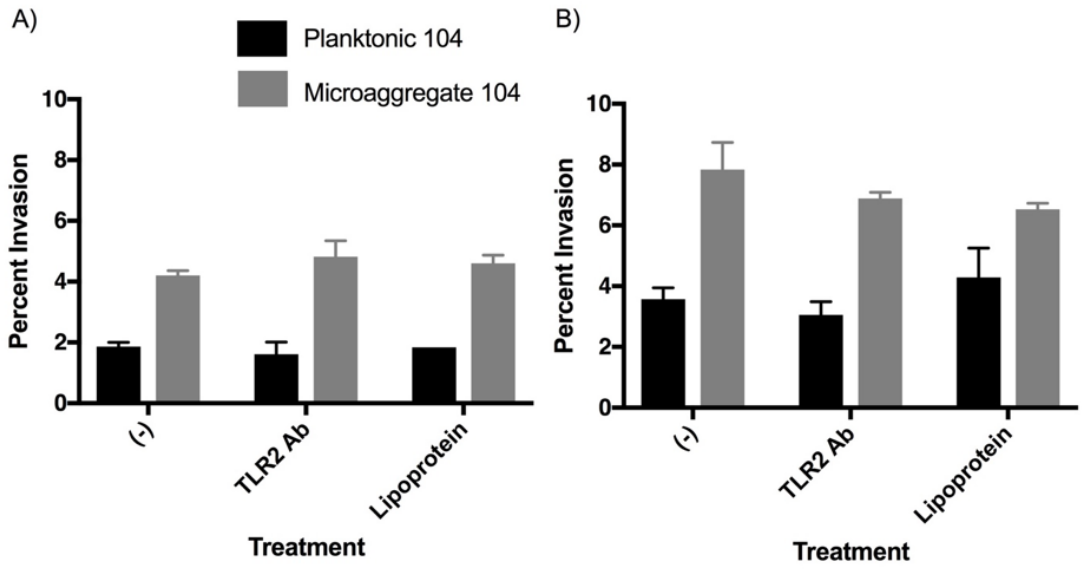

Figure 1. Neutralizing TLR2 does not affect MAH microaggregate invasion in respiratory epithelial cells. Bronchial epithelial cells (BEAS-2B) were treated with a human TLR2 neutralizing antibody, PAb hTLR2, 30 minutes prior to infection or a synthetic lipoprotein 24 hours before infection. Then cells were infected for either 1 hour (a) or 2 hours (b) with both planktonic and microaggregate phenotypes. Error bars represent standard deviation (SD). Two-sided t-tests were used, however results were not significant.

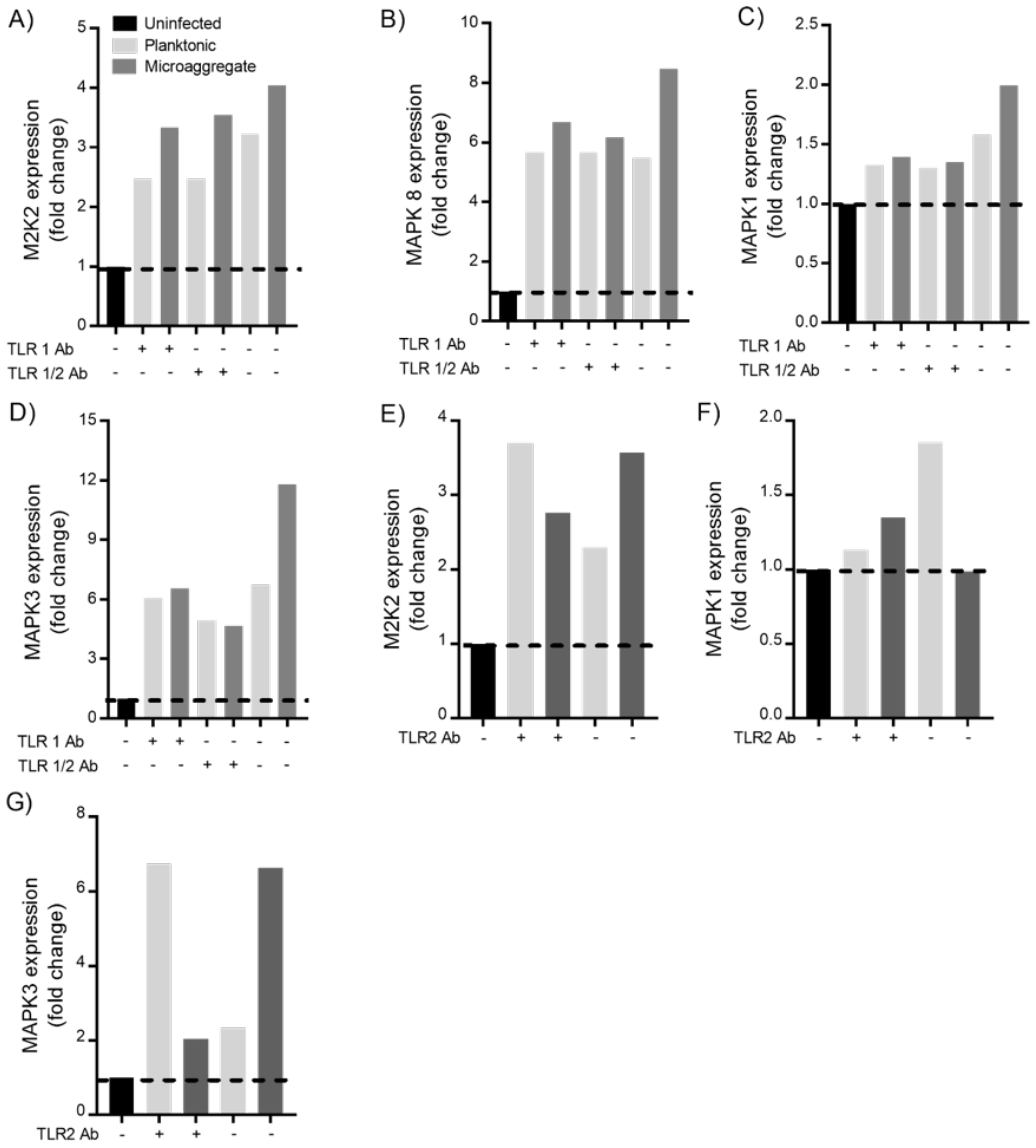

Figure 2. Real-time qPCR gene expression of MAP Kinases in bronchial epithelial cells infected with either planktonic or microaggregate bacteria. MAPK kinase 2 (M2k2), MAPK8 (JNK1), and MAPK ERK1/2 (MAPK3, MAPK1 respectively) were targeted. GAPDH was used for RNA normalization in the analysis. BEAS-2B's were either pre-treated with TLR1, TLR2, or combined TLR1/2 antibody, or no treatment before infection. All Y axes are different scales. Representative of two biological replicates.

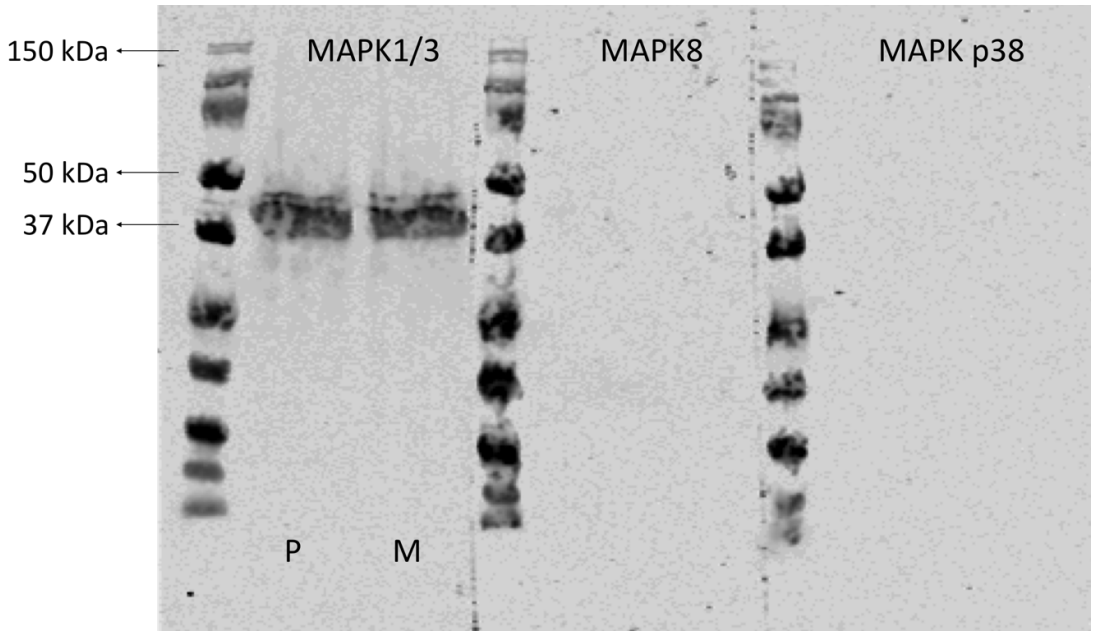

Figure 3. Western blot of phosphorylated MAP Kinase ERK 1/2 extracted from BEAS-2B cells 30 minutes post infection**.** BEAS-2B cells were infected with planktonic (P) and microaggregate (M) bacteria for 30 mins, and then lysed for phosphoprotein extraction using specific centrifugation and protein concentrators. After phosphoprotein enrichment, the remaining phosphorylated proteins were used for Western blotting with targets MAPK ERK1/2, JNK, and MAPK p38. ERK1/2 was phosphorylated, and the target sizes were 42 and 44 kD.

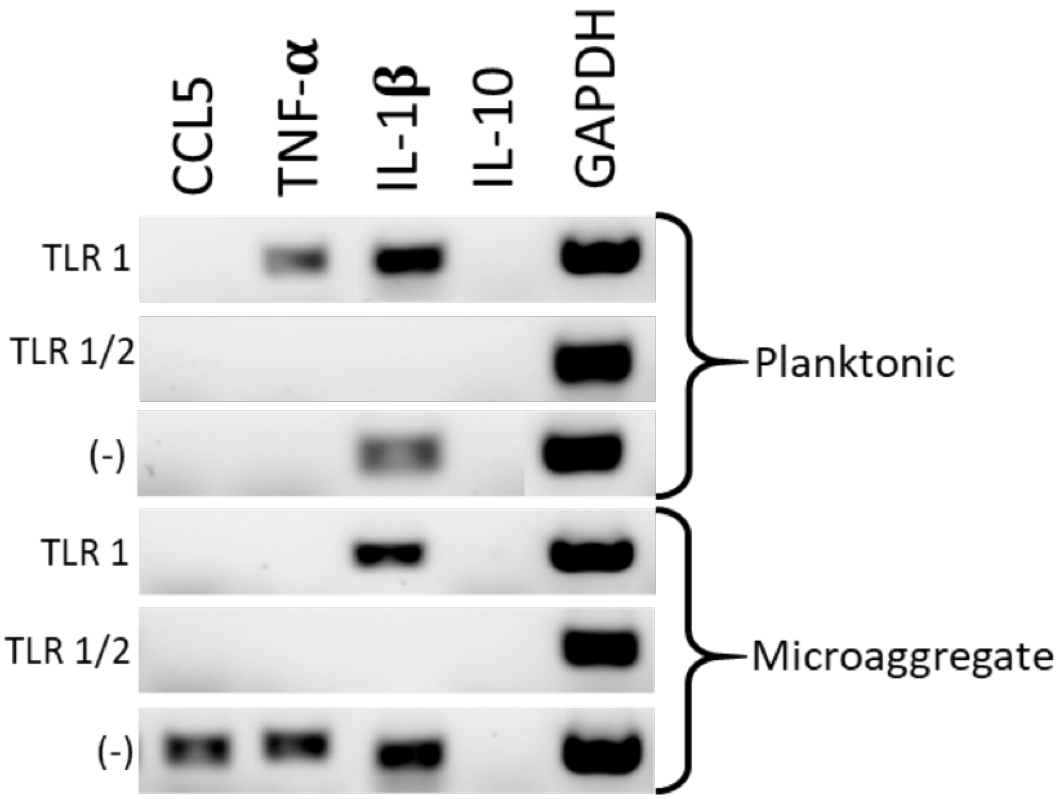

Figure 4. Cytokine and chemokine transcription is dependent on the toll-like receptor pathway in respiratory epithelial cells. Reverse-transcriptase PCR was used to determine transcriptional differences between planktonic and microaggregate infected respiratory epithelial cells with TLR1 and TLR2 neutralized. The samples used were cDNA from planktonic (A-C) or microaggregate (D-F) infected BEAS-2B cells with TLR1 neutralized (A, D), TLR1/2 neutralized(B, E), or no antibody (C, F). IL-1β, TNF-α, IL-10, and CCL5 were targeted with GAPDH used as a positive control for the PCR.

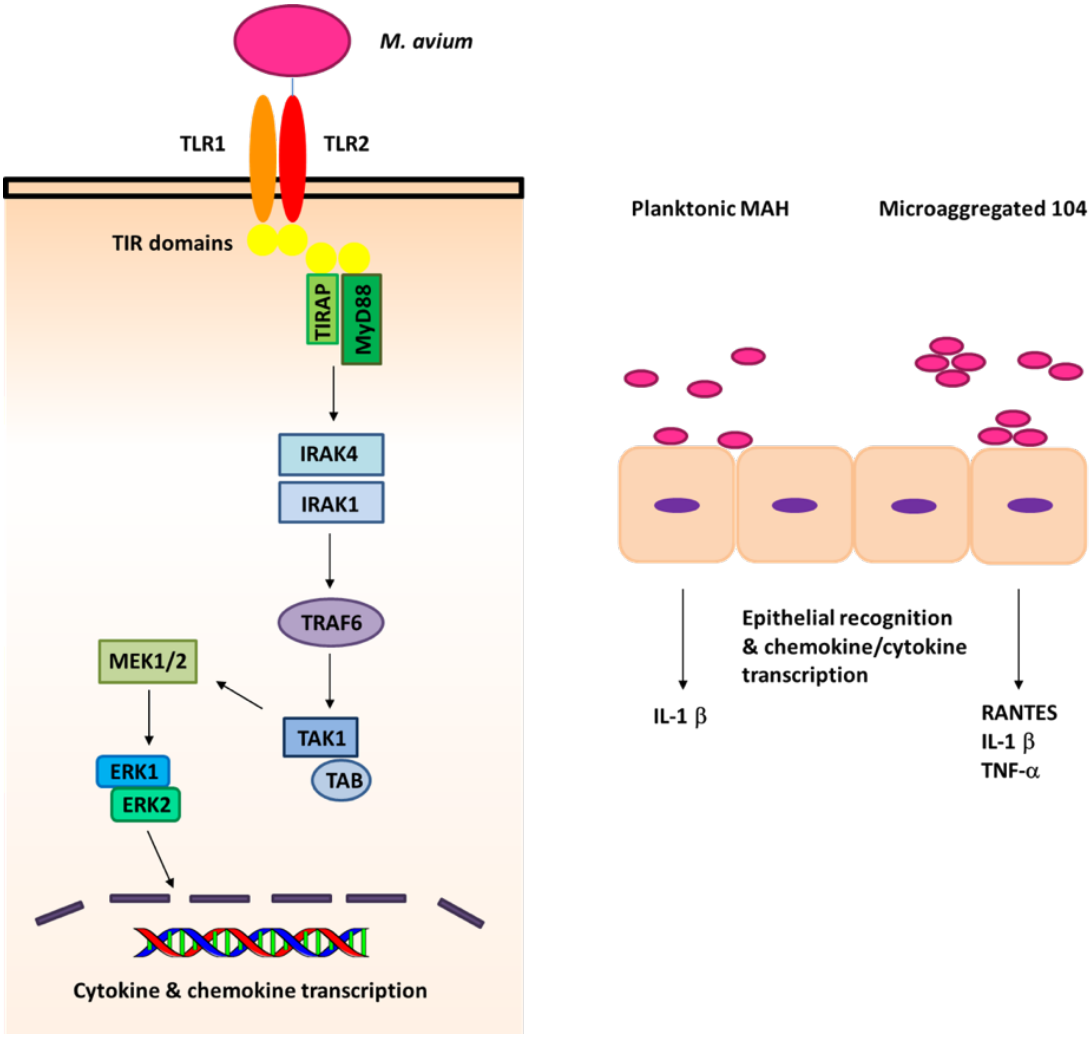

Figure 5. Depiction of the airway epithelium recognition of planktonic and microaggregated bacteria. A. Model of the intracellular toll-like receptor signaling cascade shown to be active during epithelial infection of MAH. ERK1 and ERK2 were found to be active upon infection. B. Diagram showing inflammatory molecules that have cDNA upregulated upon infection with both bacterial phenotypes.

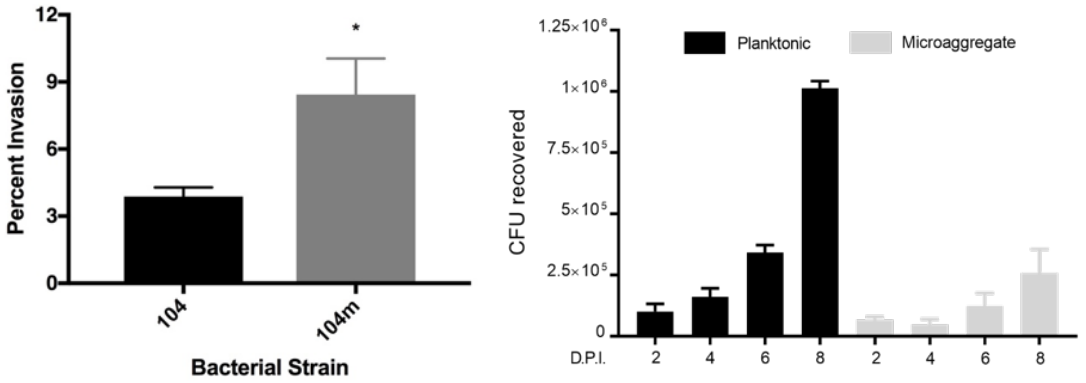

Figure 6. Planktonic (104) and microaggregate (104m) behavior within the macrophage *in vitro*. Uptake was evaluated as percent invasion (a). THP-1 cells were infected for 1 hour, treated with Amikacin at 50μg/mL for 1.5 hours to eliminate extracellular bacteria, and then lysed to determine intracellular CFUs. Representative of 5 experiments, each done in triplicate. Error bars are the calculated standard error of the mean (SEM). Subsequent time points (b) were lysed, serial diluted, and plated up to day 8 post infection to illustrate intracellular replication. Error bars show SD. Two-sided t-test, * $p < 0.05$.

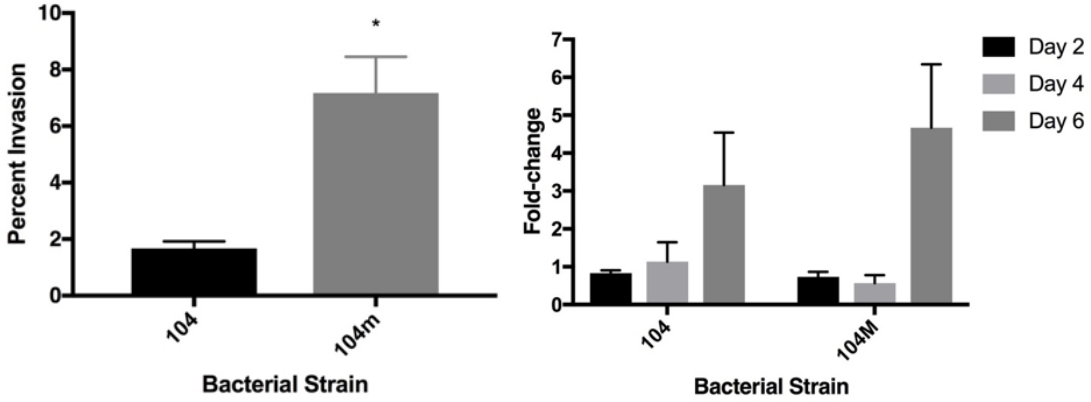

Figure 7. Uptake and survival of planktonic and microaggregate bacteria using microaggregate supernatant. During the microaggregate formation process, the bacteria is incubated in cell culture media with HEp-2 epithelial cells for 24 hours. Typically this supernatant is discarded since the monolayer is then washed with cold HBSS to capture the microaggregate bacteria. However, this supernatant was syringe filtered and then used in place of cell culture media in THP-1 uptake and survival assays. These graphs are representative of three biological replicates. Two-sided t-test, * $p < 0.05$.

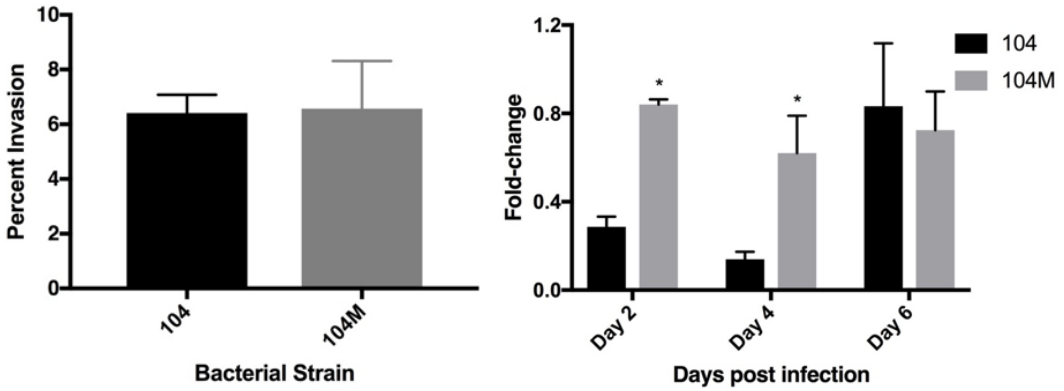

Figure 8. Uptake and survival assay using supernatant incubated with an uninfected HEp-2 cell monolayer for 24 hours. HEp-2 cell supernatant was used in place of cell culture media in the THP-1 uptake and survival assay to determine if the supernatant affect was solely a host cell response. Error bars show SD. Two-sided t-test, * $p < 0.05$.

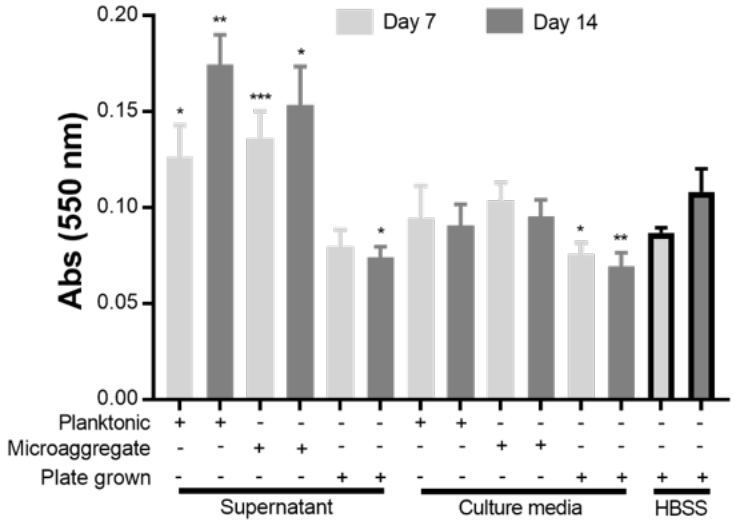

Figure 9. Biofilm mass of planktonic, microaggregate, and plate grown MAH 104 in different media conditions. Microaggregate supernatant, cell culture media, and HBSS was used to form biofilms. The crystal violet assay quantified the biofilm mass at day 7 and 14 after formation. Absorbance was normalized against the plate grown 104 in HBSS by day of formation and each treatment was performed in triplicate. Representative of two biological replicates. Error bars show SD. Two-sided t-tests, * $p < 0.05$, ** $p < 0.01$, *** $p < 0.005$.

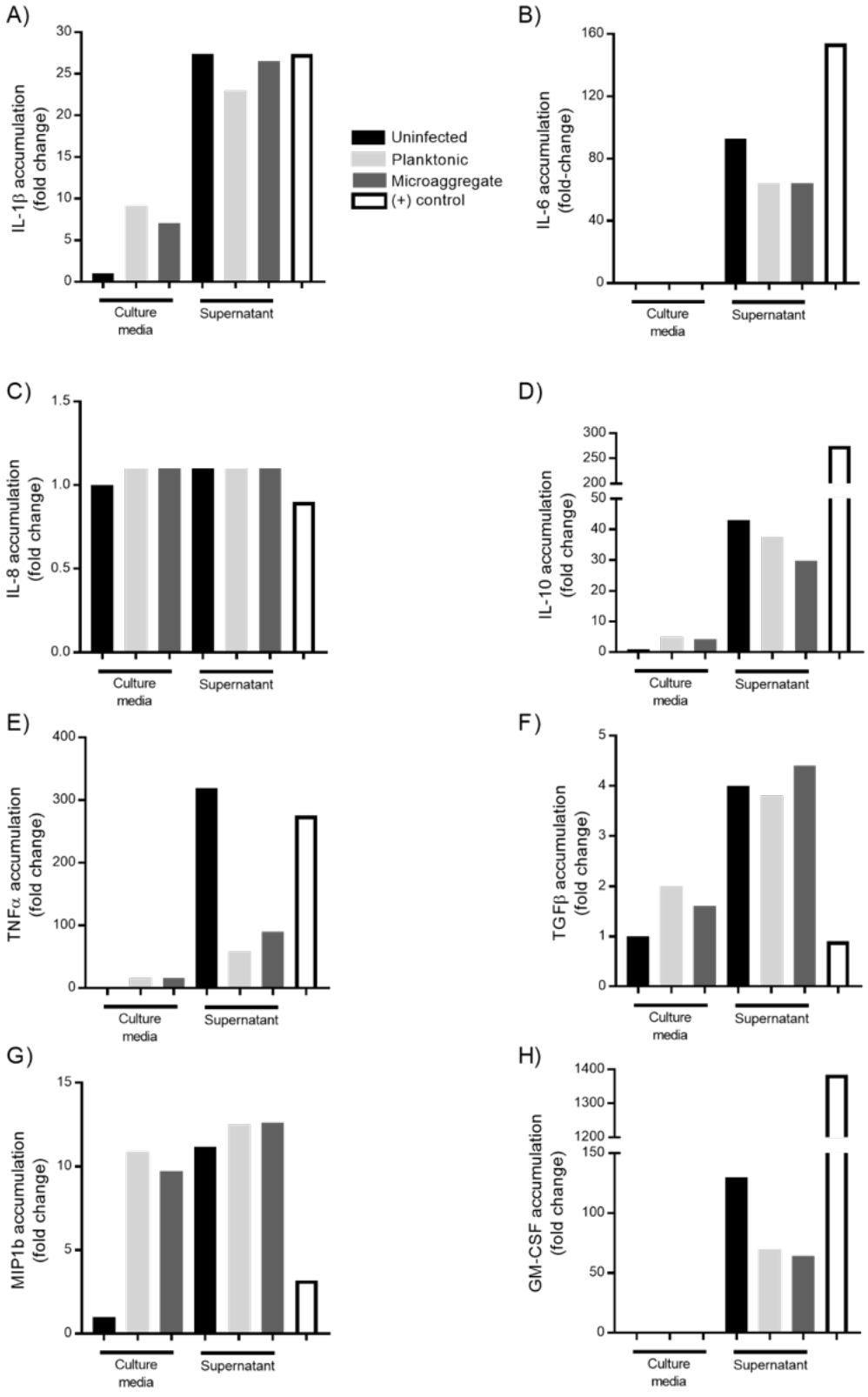
A)
IL-1β accumulation (fold change)
30
25
20
15
10
5
0
Culture media
Supernatant
Uninfected
Planktonic
Microaggregate
(+) control
B)
IL-6 accumulation (fold-change)
160
120
80
40
0
Culture media
Supernatant
C)
IL-8 accumulation (fold change)
1.5
1.0
0.5
0.0
Culture media
Supernatant
D)
IL-10 accumulation (fold change)
300
250
200
50
40
30
20
10
0
Culture media
Supernatant
E)
TNFα accumulation (fold change)
400
300
200
100
0
Culture media
Supernatant
F)
TGFβ accumulation (fold change)
5
4
3
2
1
0
Culture media
Supernatant
G)
MIP1b accumulation (fold change)
15
10
5
0
Culture media
Supernatant
H)
GM-CSF accumulation (fold change)
1400
1300
1200
150
100
50
0
Culture media
Supernatant

Figure 10. Differing cytokine secretion between microaggregate supernatant and complete media treated THP-1 cells. An ELISA was performed on 6 samples: planktonic infected cells, microagggregate infected cells, and uninfected cells with either supernatant or cell culture media 24 hours post infection. Absorbance was taken at 450 nm for the following targets: IL-1β, IL6, IL8, IL10, TNFα, TGFβ, MIP-1b, and GM-CSF. Values were compared to the uninfected cells with complete cell culture to determine fold-change. All Y axes are different scales.

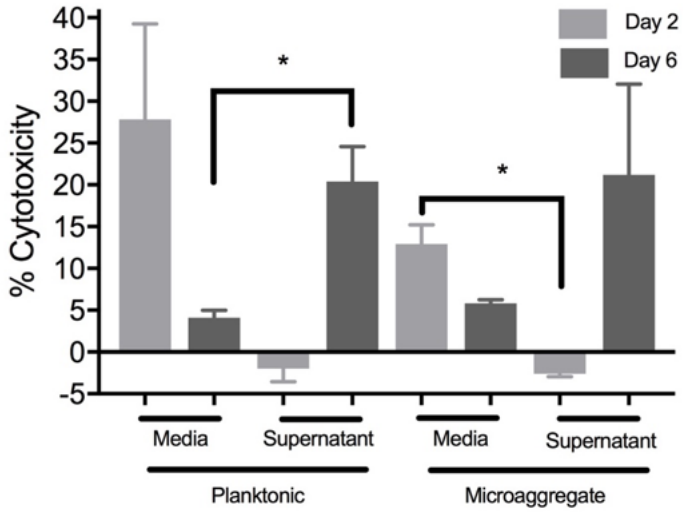

Figure 11. Cytotoxicity of macrophages upon infection with planktonic and microaggregate bacteria under complete cell culture medium and supernatant. Percent cytotoxicity was determined at day 2 and 6 post infection using the lactate dehydrogenase assay (LDH). Unpaired t tests, error bars show SD. * = $P < 0.05$

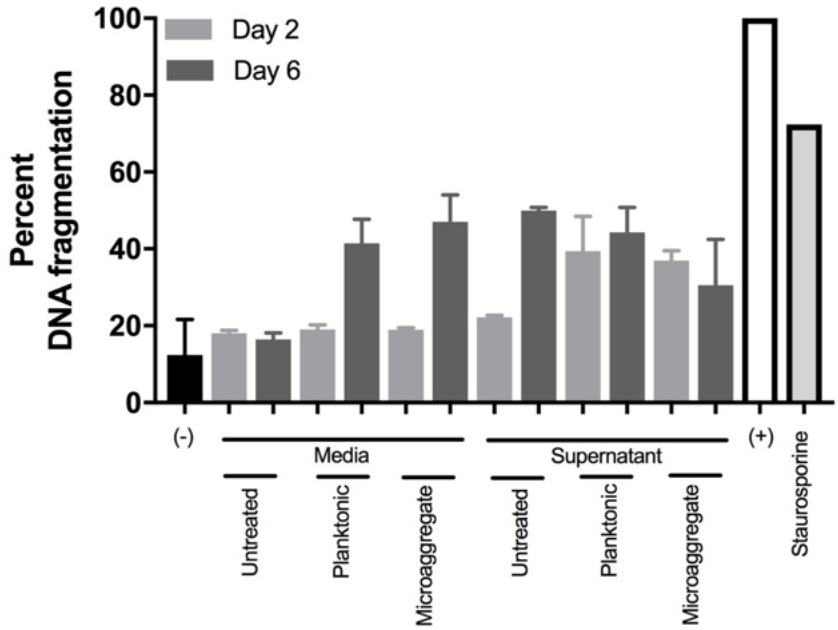

Figure 12. Percent of apoptotic DNA fragmentation as determined by Trevigen Apoptotic Cell System (TACS) by colorimetric detection in macrophages. THP-1 cells were treated with either complete culture medium or microaggregate supernatant and infected with both phenotypes. The positive control was nuclease treated cells and determined to be 100% apoptosis. Unpaired t tests were run with no significance. Error bars show SD.

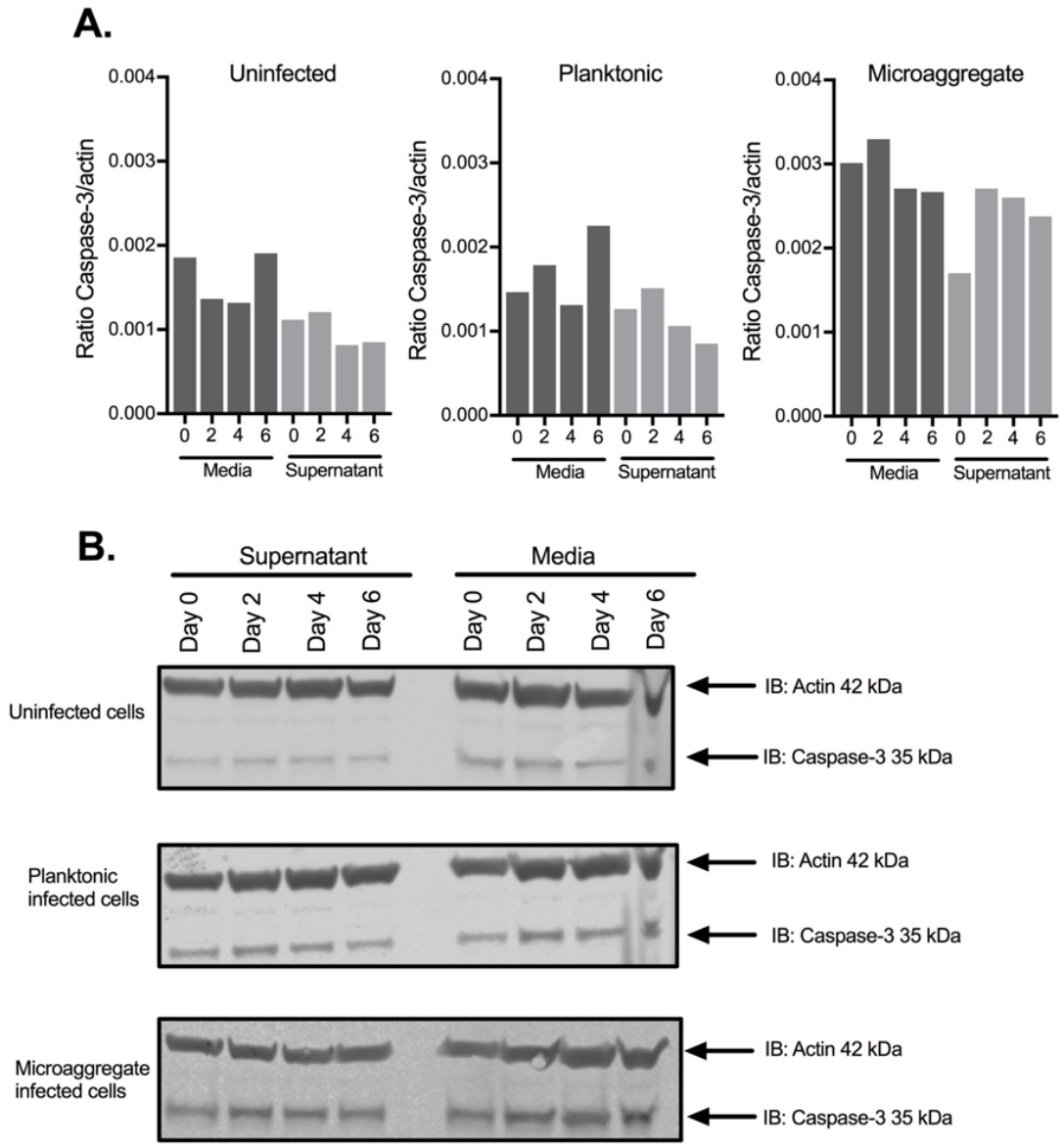

Figure 13. Western blotting for protein expression levels of Caspase-3. THP-1 cells were infected with either planktonic or microaggregates under supernatant or complete culture media condition. Monolayers were lysed after the initial infection and days 2, 4, and 6 post infection for host cell protein. Caspase-3 was targeted with β-actin as a loading control. A. Caspase-3 band intensity was divided by the loading control intensity to determine the ratio of expression change over the time course of the infection. B. Western blot image of the samples.

References

1. Stout JE, Koh W-J, Yew WW. 2016. Update on pulmonary disease due to non-tuberculous mycobacteria. Int J Infect Dis 45:123–134.

2. Kendall B, Winthrop K. 2013. Update on the Epidemiology of Pulmonary Nontuberculous Mycobacterial Infections. Semin Respir Crit Care Med 34:087–094.

3. McGarvey J, Bermudez LE. 2002. Pathogenesis of nontuberculous mycobacteria infections. Clin Chest Med 23:569–583.

4. Yamazaki Y, Danelishvili L, Wu M, Hidaka E, Katsuyama T, Stang B, Petrofsky M, Bildfell R, Bermudez LE. 2006. The ability to form biofilm influences Mycobacterium avium invasion and translocation of bronchial epithelial cells. Cell Microbiol 8:806–814.

5. Babrak L, Danelishvili L, Rose SJ, Kornberg T, Bermudez LE. 2015. The Environment of "Mycobacterium avium subsp. hominissuis" Microaggregates Induces Synthesis of Small Proteins Associated with Efficient Infection of Respiratory Epithelial Cells. Infect Immun 83:625–636.

6. Babrak L, Danelishvili L, Rose SJ, Bermudez LE. 2015. Microaggregate-associated protein involved in invasion of epithelial cells by *Mycobacterium avium* subsp. *hominissuis*. Virulence 6:694–703.

7. Lien E, Sellati TJ, Yoshimura A, Flo TH, Rawadi G, Finberg RW, Carroll JD, Espevik T, Ingalls RR, Radolf JD, Golenbock DT. 1999. Toll-like Receptor 2 Functions as a Pattern Recognition Receptor for Diverse Bacterial Products. J Biol Chem 274:33419–33425.

8. Takeuchi O, Sato S, Horiuchi T, Hoshino K, Takeda K, Dong Z, Modlin RL, Akira S. 2002. Cutting Edge: Role of Toll-Like Receptor 1 in Mediating Immune Response to Microbial Lipoproteins. J Immunol 169:10–14.

9. Akira S, Takeda K. 2004. Toll-like receptor signalling. Nat Rev Immunol 4:499–511.

10. Diamond G, Legarda D, Ryan LK. 2000. The innate immune response of the respiratory epithelium. Immunol Rev 173:27–38.

11. Gomes MS, Flórido M, Cordeiro JV, Teixeira CM, Takeuchi O, Akira S, Appelberg R. 2004. Limited role of the Toll-like receptor-2 in resistance to Mycobacterium avium. Immunology 111:179–185.

12. Rocco JM, Irani VR. 2011. <I>Mycobacterium avium</I> and

modulation of the host macrophage immune mechanisms [Review article]. Int J Tuberc Lung Dis 15:447–452.

13. Collins AC, Cai H, Li T, Franco LH, Li X-D, Nair VR, Scharn CR, Stamm CE, Levine B, Chen ZJ, Shiloh MU. 2015. Cyclic GMP-AMP Synthase Is an Innate Immune DNA Sensor for Mycobacterium tuberculosis. Cell Host Microbe 17:820–828.

14. Ogura N, Tobe M, Sakamaki H, Nagura H, Hosaka H, Akiba M, Abiko Y, Kondoh T. 2004. Interleukin-1beta increases RANTES gene expression and production in synovial fibroblasts from human temporomandibular joint. J Oral Pathol Med 33:629–633.

15. Carter G. 2003. Characterization of biofilm formation by clinical isolates of Mycobacterium avium. J Med Microbiol 52:747–752.

16. O'Toole GA. 2011. Microtiter Dish Biofilm Formation Assay. J Vis Exp.

17. Nguyen M-T, Peisl L, Barletta F, Luqman A, Götz F. 2018. Toll-Like Receptor 2 and Lipoprotein-Like Lipoproteins Enhance *Staphylococcus aureus* Invasion in Epithelial Cells. Infect Immun 86.

18. Babrak L, Bermudez LE. 2018. Response of the respiratory mucosal cells to mycobacterium avium subsp. Hominissuis microaggregate. Arch Microbiol 200:729–742.

19. Mirsaeidi M, Machado RF, Garcia JGN, Schraufnagel DE. 2014. Nontuberculous Mycobacterial Disease Mortality in the United States, 1999–2010: A Population-Based Comparative Study. PLoS ONE 9:e91879.

20. Vankayalapati R, Wizel B, Samten B, Griffith DE, Shams H, Galland MR, Fordham von Reyn C, Girard WM, J. Wallace, Jr. R, Barnes PF. 2001. Cytokine Profiles in Immunocompetent Persons Infected with *Mycobacterium avium* Complex. J Infect Dis 183:478–484.

21. Butler RE, Brodin P, Jang J, Jang M-S, Robertson BD, Gicquel B, Stewart GR. 2012. The Balance of Apoptotic and Necrotic Cell Death in Mycobacterium tuberculosis Infected Macrophages Is Not Dependent on Bacterial Virulence. PLoS ONE 7:e47573.

22. Early J, Fischer K, Bermudez LE. 2011. Mycobacterium avium uses apoptotic macrophages as tools for spreading. Microb Pathog 50:132–139.

23. Danelishvili L, McGarvey J, Li Y, Bermudez LE. 2003. *Mycobacterium tuberculosis* infection causes different levels of apoptosis and necrosis in human macrophages and alveolar epithelial cells. Cell Microbiol 5:649–660.

24. Müller A, Hacker J, Brand BC. 1996. Evidence for apoptosis of human macrophage-like HL-60 cells by Legionella pneumophila infection. Infect Immun 64:4900–4906.

25. Elmore S. 2007. Apoptosis: A Review of Programmed Cell Death. Toxicol Pathol 35:495–516.

26. Bermudez LE, Parker A, Petrofsky M. 1999. Apoptosis of Mycobacterium avium-infected macrophages is mediated by both tumour necrosis factor (TNF) and Fas, and involves the activation of caspases. Clin Exp Immunol 116:94–99.

27. Lee K-I, Whang J, Choi H-G, Son Y-J, Jeon HS, Back YW, Park H-S, Paik S, Park J-K, Choi CH, Kim H-J. 2016. Mycobacterium avium MAV2054 protein induces macrophage apoptosis by targeting mitochondria and reduces intracellular bacterial growth. Sci Rep 6.